Fluid tunnel research for challenges of urban climate

Urban Climate 51 (2023) 101659

Contents lists available at ScienceDirect

Urban Climate

journal homepage: www.elsevier.com/locate/uclim

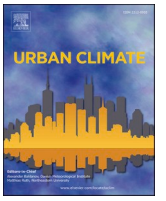

Fluid tunnel research for challenges of urban climate

Yongling Zhao [a,*], Lup Wai Chew [b], Yifan Fan [c,d], Christof Gromke [e], Jian Hang [f], Yichen Yu [g], Alessio Ricci [h,i], Yan Zhang [c,d], Yunpeng Xue [j], Sofia Fellini [k,l], Parham A. Mirzaei [m], Naiping Gao [n], Matteo Carpentieri [o], Pietro Salizzoni [k], Jianlei Niu [g], Jan Carmeliet [a]

[a] Department of Mechanical and Process Engineering, ETH Zürich, Switzerland
[b] Department of the Built Environment, National University of Singapore, Singapore
[c] College of Civil Engineering and Architecture, Zhejiang University, China
[d] International Research Center for Green Building and Low-Carbon City, Zhejiang University, China
[e] Laboratory of Building and Environmental Aerodynamics, Institute for Hydromechanics, Karlsruhe Institute of Technology, Germany
[f] School of Atmospheric Sciences, Sun Yat-Sen University, China
[g] Department of Building Environment and Energy Engineering, Hong Kong Polytechnic University, Hong Kong, China
[h] University School for Advanced Studies IUSS, Italy
[i] Eindhoven University of Technology, the Netherlands
[j] Future Resilient Systems, Singapore-ETH Centre, ETH Zurich, Singapore
[k] Univ Lyon, INSA Lyon, CNRS, Ecole Centrale de Lyon, Univ Claude Bernard Lyon 1, France
[l] Department of Environment, Land and Infrastructure Engineering, Politecnico di Torino, Italy
[m] Department of Civil and Architectural Engineering, Aarhus University, Denmark
[n] Department of Mechanical Engineering, Tongji University, China
[o] Department of Mechanical Engineering Sciences, University of Surrey, United Kingdom

ARTICLE INFO

Keywords:
Fluid tunnel measurements
Field measurements
Multiphysics urban climate processes
Scaled indoor/outdoor measurements

ABSTRACT

Experimental investigations using wind and water tunnels have long been a staple in fluid mechanics research. These experiments often choose a specific physical process to be investigated, whereas studies involving multiscale and multiphysics processes are rare. In the era of climate change, there is increasing interest in innovative experimental studies in which fluid (wind and water) tunnels are used in the modeling of multiscale, multiphysics phenomena of the urban climate. Fluid tunnel measurements of urban-physics-related phenomena are also required to facilitate the development and validation of advanced multiphysics numerical models. As a repository of knowledge for modeling these urban processes, we cover the fundamentals, experimental design guidelines, recent advances, and outlook of eight selected research areas, i.e., (i) absorption of solar radiation, (ii) inhomogeneous thermal buoyancy effects, (iii) influence of thermal stratification on land-atmosphere interactions, (iv) indoor and outdoor natural ventilation, (v) aerodynamic effects of vegetation, (vi) dispersion of pollutants, (vii) outdoor wind thermal comfort, and (viii) wind flows over complex urban sites. Three main challenges are discussed, i.e., (i) the modeling of multiphysics, (ii) the modeling of anthropogenic processes, and

* Corresponding author.
E-mail addresses: yozhao@ethz.ch (Y. Zhao), lupwai@nus.edu.sg (L.W. Chew), yifanfan@zju.edu.cn (Y. Fan), gromke@kit.edu (C. Gromke), hangj3@mail.sysu.edu.cn (J. Hang), yichen.yu@polyu.edu.hk (Y. Yu), a.ricci@tue.nl (A. Ricci), 12012029@zju.edu.cn (Y. Zhang), yunpeng.xue@sec.ethz.ch (Y. Xue), sofia.fellini@ec-lyon.fr (S. Fellini), parhammir@cae.au.dk (P.A. Mirzaei), gaonaiping@tongji.edu.cn (N. Gao), m.carpentieri@surrey.ac.uk (M. Carpentieri), pietro.salizzoni@ec-lyon.fr (P. Salizzoni), jian-lei.niu@polyu.edu.hk (J. Niu), cajan@ethz.ch (J. Carmeliet).

https://doi.org/10.1016/j.uclim.2023.101659
Received 10 March 2023; Received in revised form 11 July 2023; Accepted 15 August 2023
Available online 25 August 2023

(iii) the combined use of fluid tunnels and scaled outdoor and field measurements for urban climate studies.

Nomenclature

Re	Reynolds number (-)
Ri	Richardson number (-)
Ro	Rossby number (-)
Sc	Schmidt number (-)
Gr	Grashof number (-)
Fr	Froude number (-)
Pe	Peclet number (-)
Je	Jensen number (-)
M	geometric scale factor (-)
Δ	the change (-)
R	radiative heat flux (W m^{-2})
G	ground heat flux (W m^{-2})
S	sensible heat flux (W m^{-2})
RI	radiation intensity (W m^{-2})
ET	evapotranspiration rate (k $s^{-1}m^{-2}$)
U	freestream fluid (bulk) velocity (m s^{-1})
$\widetilde{U}$	velocity scale (m s^{-1})
F	momentum (kg m s^{-1})
p	pressure (Pa)
D	urban diameter (m)
CD	characteristic dimension (m)
N	buoyancy frequency (s^{-1})
T	temperature (K)
H	length scale in vertical direction (m)
W	width scale in streamwise direction (m)
z	vertical coordinate (m)
d	porous sample thickness in streamwise direction (m)
g, $g^{'}$	gravitational constant, reduced gravity (m s^{-2})
c_P	specific heat capacity (J kg^{-1} K^{-1})
A	surface area (m^2)
AI	area index (-)
VF	view factor (-)
TI	turbulence intensity (-)
m, n	regression coefficient (-)
CHTC	convective heat transfer coefficient (-)

Greek letters

β	fluid thermal expansion rate (K^{-1})
θ	potential temperature (K)
λ	pressure loss coefficient (m^{-1})
ν	kinematic viscosity (m^2 s^{-1})
κ	diffusivity (m^2 s^{-1})
ρ	fluid density (kg m^{-3})
Ψ	latent heat of vaporization (J g^{-1})
σ	Stefan-Boltzmann constant (W m^{-2} K^{-4})
ξ	turbulence length scale (m)
ε	emissivity (-)
ψ	steepness of two neighboring street canyons (-)

Subscripts

L	surface length-based characteristics
b	bulk characteristics
fs	full scale

ms	model scale
hs	human scale (body or segment)
fa	frontal area
pa	planar area
ed	extracted drag
af	approaching flow
N	net (all-wave) radiation
S	sensible
rs	radiative surface
tp	thermopile
sw	shortwave
lw	longwave
0	reference
st	static (pressure)
dyn	dynamic (pressure)
wwd	windward
lwd	leeward
pdl	pedestrian level

1. Introduction

Wind tunnels have been an indispensable tool in advancing mankind's technology, from the Wright Brothers' Flyer to Neil Armstrong's statement during the Apollo 11 moon mission, i.e., "One small step for man, one giant leap for mankind". Even with today's advanced computational power and the popularity of computational fluid dynamics (CFD), wind tunnel experiments are still used extensively due to their good capability and feasibility. As a result, such experimental studies still are considered to be irreplaceable in fluid mechanics research, especially in dealing with complex flow mechanisms. While the contribution of wind tunnels in rocket science (literally) is well known, this experimental approach also is essential in other areas of research, including wind engineering, urban physics, sports engineering, and many others. Water tunnels serve the same purpose in experimental fluid mechanics and offer some advantages for studies of the urban climate, such as the possibility of measuring non-isothermal flow fields at a high spatial resolution and reducing the sizes of models because of the higher viscosity of water compared to air. Both air and water are fluids, and the physics are governed by the same equations, namely the Navier-Stokes equations. Therefore, in this paper, we used the term "fluid tunnel" to cover both wind tunnels and water tunnels. Other types of fluids, such as glycerol, can be used in fluid tunnels (McPhail et al., 2015; Chang et al., 2021), but they are less common so they are not discussed in this paper.

Fluid tunnel experiments for urban climate research have had to use scaled-down models due to the limitations of the dimensions of the fluid tunnel test section. One commonly asked question concerns the size of a fluid tunnel that is required for modeling a realistic, full-scale urban climate problem (Meroney, 2016). Are we able to capture the same physics at full scale using building models with a scaled-down ratio of 1:10? What about ratios of 1:100, 1:1000, and others? Similarities or dimensional analysis in fluid mechanics can provide key dimensionless parameters that are important for a specific application; however, these dimensionless parameters often cannot be matched simultaneously in measurements. Therefore, care should be taken when applying the results of fluid tunnel experiments to full-scale applications. CFD can complement this weakness of scaling mismatches in fluid tunnel experiments by using full-scale simulations (Blocken, 2014). This raises another question that is commonly asked, i.e., why do we still use fluid tunnels despite great advances in CFD and computational resources (Meroney, 2016). The answer could be that the mutual and complementary use of these techniques guarantees enhanced performance by leading to a better understanding and interpretation of the underlying physics (Murakami, 1990; Stathopoulos, 1997; Li et al., 2006; Blocken, 2014). It is worth noting that the parameterization of thermal and vapor fluxes at the boundaries of complex geometries continues to be a challenge for CFD. There are many high-quality reviews and guidelines for the use of CFD in urban physics and, more specifically, in urban climates (e.g. Franke et al., 2007; Tominaga et al., 2008; Britter and Schatzmann, 2010; Blocken and Gualtieri, 2012; García-Sánchez et al., 2018); however, such reviews and guidelines are lacking for the applications of fluid tunnels in urban climate analysis. Therefore, this paper addresses the capabilities and challenges of fluid tunnel applications in urban climates.

The working principle of fluid tunnels is rather simple, i.e., the fluid is driven in bulk by fans or pumps to generate a flow that usually is steady or quasi-steady across the test section. This method of generating flows has the advantage of easy and accurate control of the flow rate (and hence velocity), and the use of wire meshes, screens, and honeycombs can reduce the undesirable turbulence of the flow (e.g. Groth and Johansson, 1988; Kulkarni et al., 2011). A fluid tunnel can be an open or a closed loop. In an open-loop fluid tunnel, the inflow and outflow are not connected; therefore, a smaller space is required. In a closed-loop fluid tunnel, the fluid from the outflow recirculates back to the inflow by completing a 360-degree return circuit through multiple turns. Therefore, a closed-loop fluid tunnel requires a larger space and is more difficult to design due to potential flow separations at the turnings; however, such a tunnel has the major advantage of lower operating costs because the fluid is recirculated. In addition to the basic setup of a fluid tunnel experiment, the three major requirements for urban climate modeling in fluid tunnels are (1) the generation and development of a desired atmospheric boundary layer (ABL), (2) generation of heated fluxes from objects of interest, and (3) generation of scalar

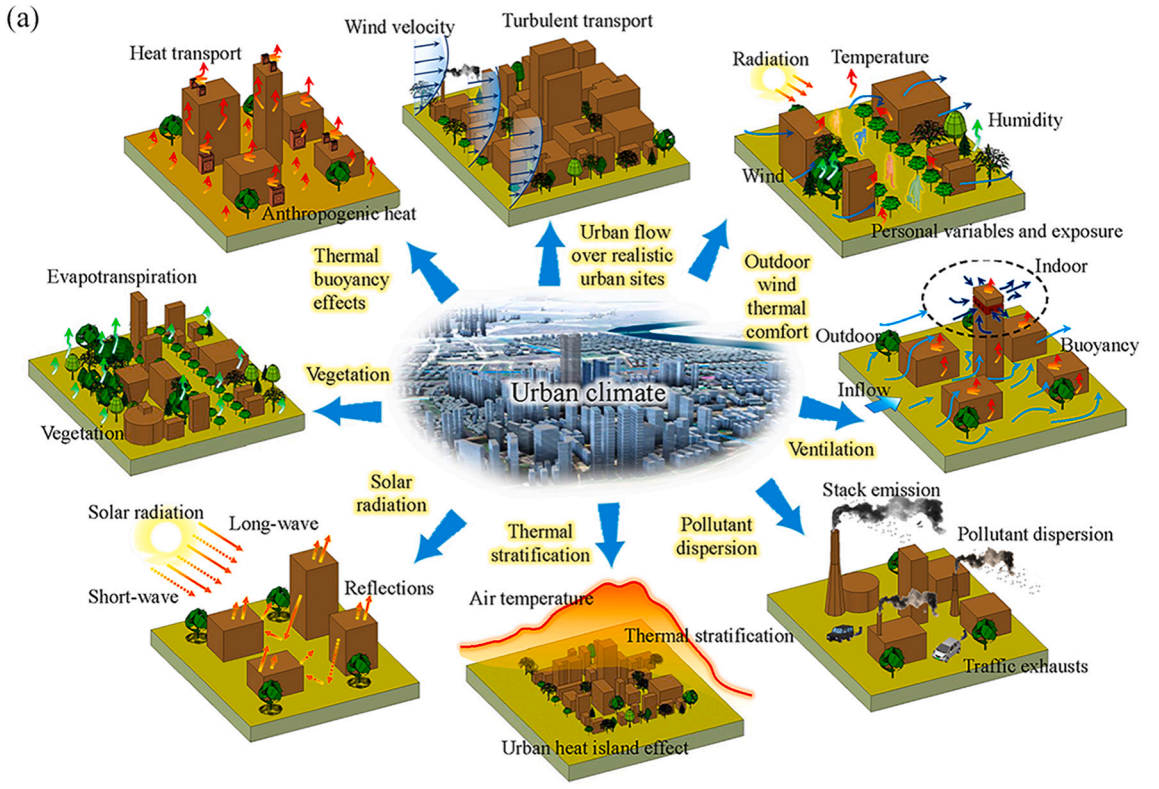

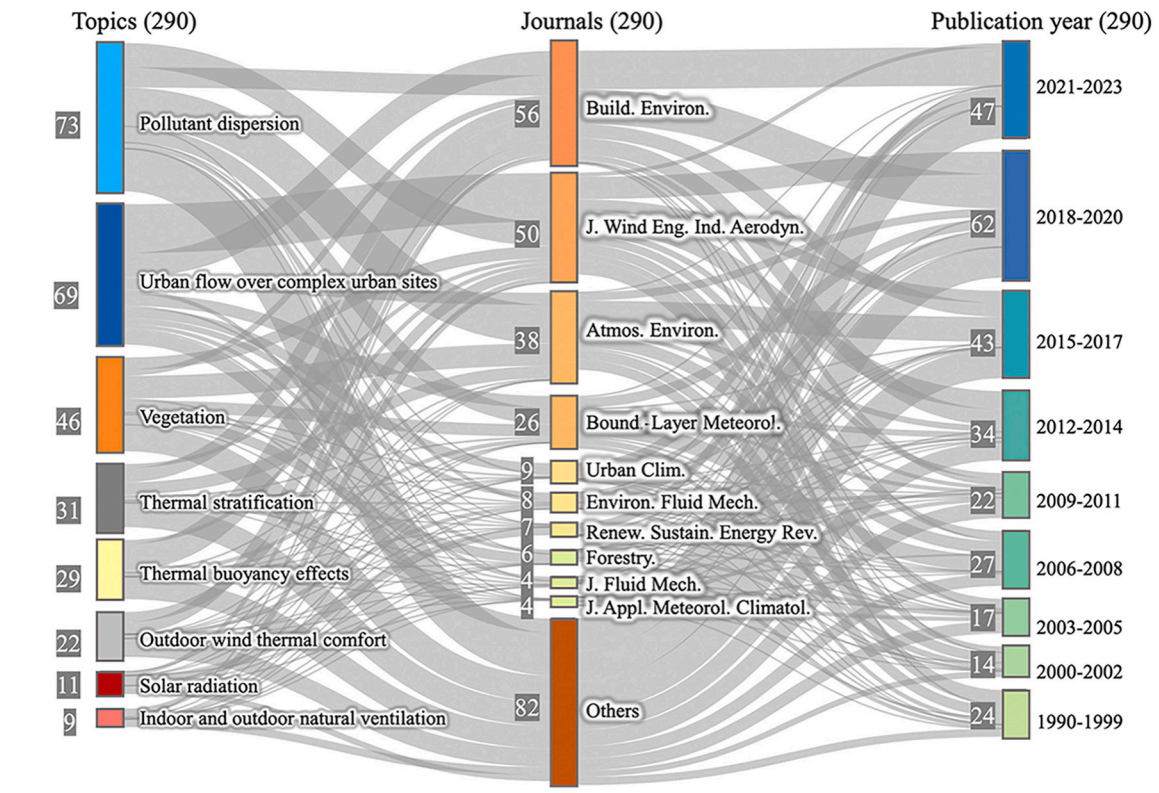

(caption on next page)

Fig. 1. (a) Fluid tunnel modeling capabilities for physical processes of the urban climate and (b) bibliometrics of the eight connected urban climate topics.

transport. First, to achieve a fully developed approach to neutral ABL flow following a log-law or power law (Stull, 1988), the roughness fetch and vortex generators can be arranged upstream from the scaled model (e.g. Castro and Robins, 1977; Chew et al., 2017; Zhang et al., 2017; Catarelli et al., 2020). Second, to simulate heated surfaces, such as streets and the exterior walls of buildings that are heated by solar radiation, heating elements must be integrated into the fluid tunnel without obstructing the flow (e.g. Allegrini et al., 2013; Cui et al., 2016; Zhao et al., 2022b). Third, the modeling of scalar transport, such as pollutant dispersion, requires the release (and purging) of tracer gas or particles in fluid tunnels (e.g. Meroney et al., 1996; Liu et al., 2010; Gromke and Ruck, 2012; Fellini et al., 2022).

When these requirements are fulfilled, fluid tunnels can realistically reproduce and model the multiphysical processes of the urban climate. As depicted in Fig. 1a, the eight key multiphysics research areas commonly studied in fluid tunnels are covered in this study. A bibliometrics based on 290 literatures reviewed in this paper is also presented in Fig. 1b to show the topics, top 10 publication journals and year of publication. The topics have primarily focused on pollutant dispersion, urban flow over complex urban sites, vegetation, thermal stratification and thermal buoyancy effects. It is also evident that fluid tunnel research of urban climate topics has been receiving increasing interest since 2000. The parameters of interest of these topics and their ranges that have been studied for each topic are summarized in Table 1. Other rare but important applications of fluid tunnels, such as the modeling of extreme events (such as tornadoes and downburst winds), snow, rain, noise, fire, and wind-induced vibration, are not covered in this paper.

The eight research topics presented in Table 1 are ordered such that they are easy for readers to follow. Solar radiation (Section 2.1) is the main source that controls the urban surface energy budget, and it drives many processes in built environments. The presence of inhomogeneous thermal buoyancy effects (Section 2.2) in built environments is caused primarily by the absorption/release of solar radiation and anthropogenic heat generation. Thermal stratification (Section 2.3) may be established further when buoyancy effects develop differently along the height direction, which affects wind and heat transfer in cities. Buoyancy and wind can also induce natural ventilation (Section 2.4). To mitigate excessive urban heat, urban vegetation (Section 2.5) has become popular in many cities as a means of providing shade, transpirative cooling, and modification of mean flow (wind). The presence of vegetation and buoyancy effects, in turn, lead to more complex dispersion of pollutants (Section 2.6) in cities. Therefore, indoor and outdoor ventilation of venues in realistic urban sites must be understood from the perspectives of thermal comfort and air quality. Outdoor thermal comfort (Section 2.7), which depends on thermal conditions and wind speeds, is an important consideration for the design of buildings and urban planning. Finally, the knowledge derived from each research area can be culminated in modeling flows across realistic, complex urban sites (Section 2.8).

In each section, fundamental considerations are provided first, and these considerations are followed by recommendations for the design of experiments, recent advances, and an outlook. The remainder of the paper is organized as follows: Section 2 describes the main advances in fluid tunnel modeling of the multiphysics of the urban climate; Section 3 focuses on three main challenges for fluid tunnel modeling of the urban climate; and Section 4 presents the conclusions and remarks.

2. Advances in modeling of multiphysics of urban climate

2.1. Modeling of solar radiation

2.1.1. Fundamental considerations

The net amount of radiant energy (R_N) on urban surfaces, along with the distribution among sensible heat flux (S), latent heat flux (ΨET) and ground heat flux (G), determine urban heat in the urban canopy layer. The simplified energy budget can be expressed as Eq. (2.1-2) (Sellers et al., 1997):

Table 1
The eight topics to be discussed in detailed in Sections 2.1–2.8

Section	Topics	Parameters of interest	Visited ranges of parameters
2.1	Solar radiation	• Re_L (surface length based) • RI	• $10^4 < Re_L < 8 \times 10^4$ • $50 < RI < 200$ (W m^{-2})
2.2	Inhomogeneous thermal buoyancy effects	• Ri_b • H/W	• $-0.21 < Ri_b < 4.44$ • $0.67 < H/W < 2.3$
2.3	Thermal stratification	• Fr	• $0.03 < Fr < 0.08$
2.4	Indoor and outdoor natural ventilation	• Re • Pe	• $Re > 1000$ • $Pe > 1000$
2.5	Vegetation	• λ_{fs}	• $0.5 \leq \lambda_{fs} \leq 7.8$
2.6	Pollutant dispersion	• H/W, AI_{fa}, AI_{pa} • Ri	• $0.125 < H/W < 2$ • $0.1 < AI_{fa}\langle AI_{pa}\rangle\langle 0.7$, $0.4 < Ri < 30$
2.7	Outdoor wind thermal comfort	• U • TI	• $0 < U < 13$ m/s • $0 < TKE < 30\%$
2.8	Wind flows over complex urban sites	• M • U	• $1:100 < M < 1:2000$ • $1.5 < U < 30$ m/s

Fig. 2. (a) Schematic of short- and long-wave radiation over building surfaces, (b) wind tunnel setup for measurements, and (c) solar simulators used in a wind tunnel (Mirzaei and Carmeliet, 2015).

$$R_N = S + \Psi ET + G \tag{2.1-1}$$

where Ψ is the latent heat of vaporization and ET is the evapotranspiration rate.

Shortwave and longwave radiation, as illustrated in Fig. 2a, may result in local thermal effects owing to hotspots and thermal stratification due to their diurnal changes. The local thermal effects are discussed in this section and in Section 2.2, and the thermal stratification is discussed in Section 2.3.

Radiative fluxes, in combination with convective fluxes over external surfaces, result in non-isothermal conditions in street canyons. These heat exchanges were studied by applying a heat source in fluid tunnel measurements (Cui et al., 2016; Gong et al., 2022). To realistically model both radiation and convective fluxes and avoid difficulties in the implementation of heated surfaces by artificial heaters, one can argue that using a solar simulator can technically represent radiative fluxes in fluid tunnels (Gallo et al., 2017; Li et al., 2022b). The radiation flux (R) applied in measurements can be approximated using the Stefan-Boltzmann equation (Mirzaei and Carmeliet, 2015):

$$R = VFA_{rs}\varepsilon\sigma\left(T_{rs}^4 - T_{tp}^4\right) \tag{2.1-2}$$

where VF is the view factor between the incident radiation and the surface to be measured, σ is the Stefan-Boltzmann constant, ε is the emissivity of the surface, A_{rs} is the area of the surface, T_{rs} and T_{tp} are the radiative surface and thermopile temperatures, respectively.

2.1.2. *Recommendations for the design of fluid tunnel experiments*

Reproducing solar radiation in fluid tunnels faces a wide range of challenges and barriers, which hinders the extensive adoption of such studies (Fig. 2b, c) (Mirzaei and Carmeliet, 2015). First, the choice of hot-wire anemometer, the location of the probe, and the way it is protected against radiation are of paramount importance. Probe surfaces can be covered with aluminum foils, which can be an effective strategy for other building model surfaces manufactured with materials of low melting points. Second, solar simulators generating radiative flux with one or multiple lamps should be selected based on the desired heat flux in the measurements (Tawfik et al., 2018). Placing one or multiple lamps as a solar simulator may cause non-uniform heat flux at the target surface, which is due to the shape of the lamp units, even though a more effective design can reduce this discrepancy. Thus, it is essential to monitor the spatial uniformity of radiation on a target surface using sensors, such as thermopiles (Renné, 2016). Third, a range of safety considerations must be considered. While excess surface temperature may not occur at high airflow velocities, fire risk may occur when the operating velocity in a fluid tunnel is considerably decreased when studying low wind conditions.

2.1.3. *Recent advances and outlook*

Experimental studies of solar radiation using fluid tunnel measurements are rare. Only a few studies have explored heat absorption by rooftops in scaled models. Mirzaei and Carmeliet (2015) revealed that roof-installed PV panels at $Re_L = 8\times10^4$ reached 71.9°C when there is no gap beneath the PV panels exposed to a radiation intensity of RI=200 W/m^2, while the temperature can be reduced to 56.9°C using a cavity height of 30 mm. For low rise buildings, the presence of PV panels may lead to severe local hotspots. Thorough parametric studies concerning the impact of emissivity of rooftop materials, radiation intensity, strength of convective flow, and many other factors are not yet available. The redistribution of incoming radiant heat flux to different heat flux components, which is determined by a combination of emissivity, heat capacity, and convective heat transfer coefficient of the target surfaces, is important, complex, and worthy of study. Much broader ranges of radiation intensity, wind speed and building material characteristics, as summarized in Table A1 in the appendix, can be explored to better understand heat transport and storage at various scales. The change in latent heat on target surfaces, such as evaporation-induced latent heat variation on wetted porous pavements, can also be studied.

In future studies, particle image velocimetry (PIV) can be combined with temperature measurements to understand the development of the flow field. It should be noted that the PIV technique has a relatively small laser beam area, which might not be sufficiently large to observe the entire domain of the flow. In such cases, focusing the PIV in multiple smaller planes and combining them can be a potential solution, especially when the use of hot wires in small areas can disturb the flow (Mirzaei et al., 2014). Thermography techniques can be used as an advanced technology to observe surface temperatures in large and atmospheric fluid tunnels (Le Sant et al., 2002; Mirzaei and Carmeliet, 2015).

2.2. Modeling of inhomogeneous thermal buoyancy effects

2.2.1. Fundamental considerations

The absorption of solar radiation and convective heat transfer at the surfaces of the built environment often induce inhomogeneous thermal buoyancy. As urban wind flows over asphalt pavements, building facades, or roofs at high surface temperatures due to solar radiation absorption, they are heated up and thus gain inhomogeneous thermal buoyancy through convective heat transfer. The thermal buoyancy of urban airflow can play a vital role in pollutant dispersion, heat removal, and thermal comfort of residents (e.g. Dallman et al., 2014; Mei and Yuan, 2022; Mouzourides et al., 2022).

To characterize the non-isothermal urban airflow involving convective heat transfer from urban surfaces (e.g. ground, facades, etc.), the overall process can be regarded as an approximation of a Rayleigh-Bénard-type convection subject to the shear of a horizontal wind, where the Rayleigh-Bénard-type convection can be characterized by the Grashof number, and the turbulence of the approaching horizontal wind can be approximated at a rate proportional to Re^2. Therefore, the dominance between the Rayleigh-Bénard-type convection and the turbulence generated by the approaching wind can be quantified by the bulk Richardson number (Ri_b), which can be defined in Eq. (2.2-1) (e.g. Zhao et al., 2022b):

$$Ri_b = \frac{Gr}{Re^2} = \frac{g\beta H^3 \Delta T/\nu^2}{\left(U^2 H/\nu\right)^2} = \frac{g\beta H \Delta T}{U^2} \tag{2.2-1}$$

where Gr is the Grashof number characterizing the buoyancy effect, and Re is the Reynolds number reflecting the shear effect. H is the length scale of the heat source that releases heat to the ambient fluid (e.g. air), β is the thermal expansion coefficient of the fluid, g is the acceleration due to gravity, ν is the fluid kinematic viscosity, U is the freestream fluid velocity, and ΔT is the temperature difference between the heat source and the ambient. Alternatively, the dominance can be characterized using a buoyancy parameter for a street canyon with its leeward facade at high temperatures (Mouzourides et al., 2022).

Caution must be exercised when estimating Ri_b for realistic urban settings. First, when the hydrostatic pressure variation of urban airflow is considerable, for example owing to large variations in terrain elevation, the difference in potential temperature is commonly used in the calculation of Ri_b, instead of using the absolute temperature. Second, the temperature difference can be determined between the temperature of the approaching flow and the temperature on different surfaces of grounds and buildings. Flow characteristics may only be compared and generalized for studies in which Ri_b was determined based on the same type of temperature difference. Street canyons with non-uniform leeward and windward heights should also be better characterized, for instance using the steepness ratio (Zhao et al., 2021). Third, when $Ri_b \gg 1$ the flow is dominated by convection, the design of fluid tunnel measurements can focus on the match of Ri_b between the full-scale and fluid tunnel-scale flow. However, generalizable conclusions from fluid tunnel measurements can only be drawn for dominating flow structures and physical processes. Last but not the least, when $Ri_b \sim 1$ fluid tunnel measurements can be used to study the non-isothermal urban airflow by matching similarities for both buoyancy and shear effects between full-scale and fluid tunnel-scale settings because the airflow is dominated by both effects.

2.2.2. Recommendations for the design of fluid tunnel experiments

Fluid tunnels and heated building models have been extensively used to reproduce inhomogeneous thermal buoyancy in urban airflows at reduced scales (e.g. Allegrini et al., 2014; Tsalicoglou et al., 2020). An example of the experimental setup is shown in Fig. 3a, where conductive models in water tunnels can be placed on heating power-controlled heating plates (Fig. 3b-c) to mimic heat sources in an urban climate. In the design of such experiments, particular attention needs to be paid to controlling the heating of the models. The heating of the model surfaces can be designed in two ways: constant surface temperature (Zhao et al., 2021) or constant heat flux (Gaheen et al., 2021). Uniformity of the surface temperatures must be ensured as much as possible prior to the measurements. In addition, particular caution must be paid to the height-to-width (H/W) aspect ratio of street canyons that is one of the important geometrical similarities. For extremely narrow street canyons, scaled down laboratory measurements may potentially overestimate

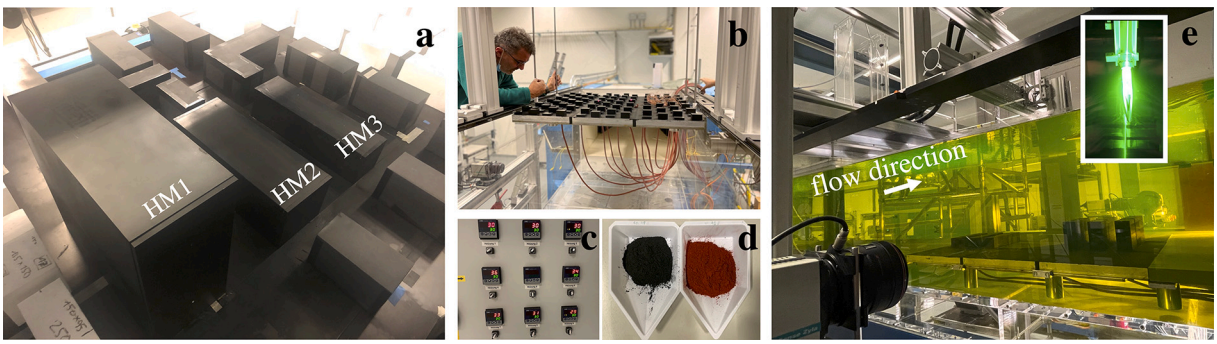

Fig. 3. Wind and water tunnel measurements of buoyancy effects of urban flows from the projects reported in Zhao et al. (2021) and Zhao et al. (2022b). (a) Wind tunnel setup showing electrically heated models (HM1-3); (b-e) Water tunnel setup showing (b) conductive models on heating plates, (c) individual controllers of heating plates, (d) fluorescence chlorophyll / uranine, and (e) optical setup.

thermal and buoyancy effects due to nonlinear growth of thermal boundary layers over building walls, which is elaborated in Zhao et al. (2020).

The design of experiments also needs to facilitate the measurements. For velocity field measurements, motorized multidimensional stages may be used to allow efficient multiple field-of-view (FOV) measurements, where lasers and the camera must be moved in a synchronized manner (Li et al., 2021a). Depending on the laser intensity and optical access to the measurement plane, a mirror may be needed to enhance the local laser intensity (Mouzourides et al., 2022).

Water tunnel measurements provide the opportunity to perform simultaneous velocity and temperature field measurements using PIV and laser-induced fluorescence (LIF)(Zhao et al., 2022b). An example of the setup is shown in Fig. 3b-e. For LIF, the fluorescence intensity measured at every pixel of the image is expected to have a linear relationship with the local laser intensity and temperature. The main challenges are the non-uniform spatial distribution of the laser sheet intensity, fluctuations in the laser intensity, and errors due to dye concentration and dye absorption (Vanderwel and Tavoularis, 2014; Zhao et al., 2022b). The uncertainties in the thermocouples used to calibrate the LIF results also limit the accuracy of the determined temperature field. Nontoxic fluorescence, such as chlorophyll and uranine (Fig. 3d), can be used for LIF measurements. LIF measurements using 1-color/1-dye or 2-color/2-dye can be adopted, depending on the desired temperature resolution(Yen et al., 2016; Zhao et al., 2022b).

2.2.3. Recent advances and outlook

Recent fluid tunnel research concerning inhomogeneous thermal buoyancy has been primarily focused on the flow developed in simplified street canyons where the Ri_b ranges from -0.21 to 4.44 (e.g. Uehara et al., 2000; Zhao et al., 2022b). The effects of the street canyon aspect ratio and buoyancy condition of the approaching flow on heat removal and mixing are revealed to some extent. However, heat removal from narrow street canyons (e.g. $H/W \gg 2.3$) or from canyons surrounded by buildings of non-uniform heights (e.g. characterized by high steepness ratio ψ), as suggested in Table A1 in the appendix, is worth future extensive studies. It is also understood that the heat removal from a street canyon to the roof-level ambient approaching flow may be doubled when the buoyancy of the approaching flow is stronger compared to the case where the street canyon is subject to an isothermal approaching flow or its buoyancy is relatively weaker. The potential impact of vegetation facades on convective heat transfer from the surfaces of building facades was also measured, and a distinct thickened stagnant layer was observed adjacent to the vegetation facades, leading to a deteriorated release of heat from buildings to the ambient environment.

In a built environment, the process of heat absorption and release through buildings and urban materials is highly time dependent, in addition to spatially inhomogeneous features. The impact of the heat capacity of building materials and the resulting time-dependent heat absorption and release, such as the heat transport in porous building materials, are much more complex and worthy of future research. In addition, reproducing direct solar radiation using solar simulators, such as the technique discussed in Section 2.1, could be integrated into future studies on hotspots and their transport in urban environments. The reproducing of stable or unstable stratified lower atmosphere also needs to be considered in studies concerning urban heat and the dispersion of fine pollutants, where buoyancy could play an important role. The experimental technique for creating thermal stratification in a fluid tunnel and the advances in the topic are discussed in Section 2.3.

2.3. Modeling of thermal stratification

2.3.1. Fundamental considerations

The stability of the ABL can be quantified using the buoyancy frequency (also called Brunt-Väisälä frequency) (Stull, 1988), N, which is defined in Eq. (2.3-1) as follows:

$$N = (g\beta\partial\theta/\partial z)^{1/2} \quad \text{2.3-1}$$

where g is gravitational acceleration, β is the fluid thermal expansion rate, θ is the potential temperature in the vertical boundary layer, z is the vertical coordinate, and $\partial\theta/\partial z$ is the potential temperature gradient. In the ABL, the typical value of N is approximately 0.015 s^{-1} (Hunt et al., 1988; Reuten, 2006).

Three physical processes cause stable stratification (Largeron and Staquet, 2016; Czarnecka and Nidzgorska-Lencewicz, 2017; Ning et al., 2018; Niedźwiedź et al., 2021). The first is a warm front over a cold front, which causes a strong temperature gradient at the interface of the two fronts and is also named elevated inversion (Largeron and Staquet, 2016). The second is due to hot air subsidence at a certain location caused by large-scale (regional or global scale) atmospheric circulation (Czarnecka and Nidzgorska-Lencewicz, 2017). The third is the radiative cooling of land surfaces at night (Ning et al., 2018; Niedźwiedź et al., 2021), which causes surface-based inversion and is the most common type of diurnal cycle. The inversions in the ABL can be caused by the joint effect of these three physical processes. The accumulation of cold air in basins or valleys can form cold pools (Clements et al., 2003; Princevac and Fernando, 2008; Vosper and Brown, 2008; Lareau et al., 2013; Yu et al., 2017) and create extremely strong inversions (N is as high as 0.1 s^{-1}).

To simulate the flow phenomenon in a stable ABL, a temperature gradient or density gradient must also be created in fluid tunnels. The non-dimensional parameters to guarantee similarities between the prototypes and reduced-scale models are Fr (Lu et al., 1997b; Cenedese and Monti, 2003; Fan et al., 2018; Fan et al., 2020; Yin et al., 2020), defined in Eq. (2.3-2) (for urban heat dome flow studies), or Ri (Ogawa et al., 1985; Uehara et al., 2000; Zhao et al., 2022a).

$$Fr = \widetilde{U} \Big/ (ND) \quad \text{2.3-2}$$

where $\widetilde{U} = [g\beta SD/(\rho_0 c_P)]^{1/3}$ is the convective velocity scale; S is the (sensible) heat flux over the simulated urban area; D is the simulated urban diameter; ρ_0 is the reference density; and c_P is the specific heat capacity.

2.3.2. Recommendations for the design of fluid tunnel experiments

There are two main methods for generating stable gradients: the use of a temperature gradient and the use of a density gradient (such as saltwater). In wind tunnels, the temperature gradient can be built by cooling the bottom and heating the top (Ogawa et al., 1981; Guo et al., 2021), which is also applicable to water tank experiments (Lu et al., 1997a; Lu et al., 1997b). Stable stratification created with saltwater can be achieved in water tank experiments using the two- bucket filling technique (Fan et al., 2018; Fan et al., 2019), as shown in Fig. 4a. There are several advantages of using saltwater. First, the density gradient can be significantly larger than that obtained with the temperature gradient method. Second, the density gradient will last longer than the temperature gradient and does not require the thermal insulation of the water tank walls and bottoms. Third, heating at the top can block the laser or light access when applying PIV to measure the velocity field, which is not a problem in setups with salt water stratifications. Fourth, density gradient profiles can be made flexible by adjusting the filling speed of salt water and pure water, for example, a neutral layer covered by a stable layer or a stable layer covered by a neutral layer (Fan et al., 2021a). If the heating method is adopted, only a linear gradient can be achieved because it utilizes heat conduction to build up the temperature gradient.

2.3.3. Recent advances and outlook

Currently, various density profiles can be obtained using the saltwater stratification method in water tank experiments. This helps to achieve the modeling of city-scale natural convection, i.e., urban heat dome flow, in water tanks. Different stratifications (stable, unstable, and neutral) can also be modeled in wind tunnels using the heating method, i.e., heating or cooling at the bottom or ceiling of the tunnel. Owing to the limitation of similarity criteria, only building/neighborhood-scale phenomena can be considered in wind tunnels.

As the frequency of heatwaves and calm weather conditions increases, buoyancy-driven flow, such as the urban heat dome in Fig. 4b, becomes increasingly important because of their impact on pollutants and heat dispersion at building and city scales (Zhao et al., 2020; Fan et al., 2021b). When background wind is absent, water tanks with stable stratifications have been used to study urban heat dome flow. However, existing studies on water tanks (1-3m in diameter) are still insufficient for simulating megacities (10-40 km in diameter). A desirable size for future studies would be 10-15m in diameter. Moreover, as the city size increases, the Coriolis force, which is quantified by the Rossby number (Ro) (Warn et al., 1995; Embid and Majda, 2006; van der Laan et al., 2020), starts to play a role in modulating buoyancy-driven flow over urban areas. In this case, a rotating water tank would be a useful tool for simulating Coriolis force-related large-scale flow structures at the city scale under Coriolis force. Temperature gradient and Coriolis force characterized by $0.01 < Fr < 0.03$ and $R_0 < 3$ are worthy of future efforts, as suggested in Table A1 in the appendix.

When the background wind is moderate and interacts with the urban heat dome flow, water channels are an important tool for simulating the approaching flow with different thermal stratifications (background density profile). The effect of non-uniform roughness and heat flux distribution within urban areas is also worthy of investigation in fluid tunnels in the future. Combining time-resolved tomographic PIV with LIF is favorable for providing high-quality 3D velocity/temperature/turbulence fields in fluid tunnel studies. Thanks to the advances made in experimental modeling of solar radiation and inhomogeneous thermal buoyancy using fluid tunnels, as well as advanced measuring technologies, urban hotspots can be reproduced and studied in fluid tunnels subject to a stratified ABL.

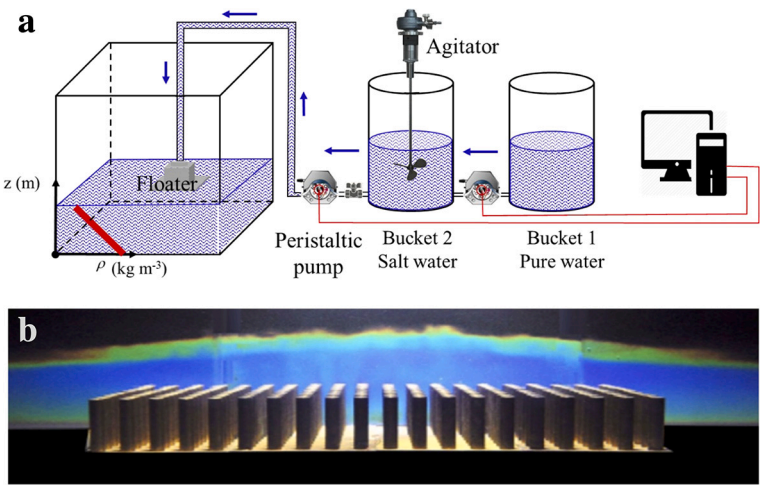

Fig. 4. (a) Illustration of the procedure for creating stable stratification with saltwater. Modified from Fan et al. (2018). (b) Temperature field, presenting a dome shape, over a reduced-scale city model in a water tank under stable stratification conditions, which was visualized by a thermochromic liquid crystal sheet (Fan et al., 2017).

2.4. Modeling of indoor and outdoor natural ventilation

2.4.1. Fundamental considerations

Natural ventilation occurs because of pressure differences arising naturally between openings in a building, which drive the exchange of air between indoor and outdoor spaces. The pressure differences can be caused by two main mechanisms: wind and buoyancy effects (or a combination of both). In both cases, the flow regime that controls the exchange of air indoors and outdoors is largely dependent on the location and geometry of the openings, pressure and temperature boundary conditions at the building envelope, and the presence of local buoyancy sources (Linden, 1999).

The pressure distributions due to wind are generally assessed through wind tunnel experiments. The nature of the urban environment and the building openings with their sharp edges makes wind speed largely irrelevant due to flow separation. This aspect simplifies the experimental investigation as it makes the problem essentially *Re*-independent (Linden, 1999). Recent studies on wind-driven flow were conducted, for example, by Ji et al. (2011), James Lo et al. (2013), Tecle et al. (2013), Shirzadi et al. (2019), Golubić et al. (2020) and Esfeh et al. (2021).

However, buoyancy-driven flows due to temperature differences may represent a challenge for fluid tunnel modeling because a lower *Re* leads to an increased importance of viscous effects (Linden, 1999). The buoyancy force can be described in terms of reduced gravity, $g^{'}$:

$$g^{'} = g\frac{\Delta\rho}{\rho} = g\frac{\Delta T}{T} \tag{2.4-1}$$

where g is the acceleration due to gravity, ρ is the density, and T is the temperature. The dimensionless numbers of concern are the Reynolds number (Re) and the Peclet number (Pe), which can be written in terms of reduced gravity as

$$Re = \frac{\sqrt{g^{'}H}\,H}{\nu};\ Pe = \frac{\sqrt{g^{'}H}\,H}{\kappa} \tag{2.4-2}$$

where ν is kinematic viscosity, κ is the coefficient of molecular diffusivity, and H is the relevant vertical scale. To reduce the mismatch in *Re* and *Pe*, small-scale experiments in water (e.g. using salinity to simulate buoyancy) are generally used (Linden et al., 1990; Davies Wykes et al., 2020). Fluid tunnel experiments can still be of value in buoyancy-driven flow, as specialized facilities might help in characterizing the temperature and heat exchange around buildings in urban areas, e.g. Marucci and Carpentieri (2019).

2.4.2. Recommendations for the design of fluid tunnel experiments

Measurements of ventilation rates in a wind tunnel are generally performed using tracer concentration techniques (Etheridge, 2011). This would require injection of a tracer gas in the building of interest for the measurement of the concentration decay due to ventilation. A fast-response instrument is then needed to capture the transient, which is typically performed using a fast-response Flame Ionization Detector (FFID), e.g. in the work of Marucci and Carpentieri (2020a). FFID can also be used for air quality studies when assessing the interactions between the interior and exterior of the building for pollution dispersion purposes.

Creating the correct wind environment is relatively easy in large boundary-layer fluid tunnels, where neutral conditions can easily be achieved in urban wind flows. Specialized facilities on the other hand, are required if non-neutral (stable or convective) boundary layers are to be generated (Marucci and Carpentieri, 2020b). As mentioned in the previous section, the correct scaling of combined wind- and buoyancy-driven flows can be particularly challenging as temperature differences between indoor and outdoor environments might have to be greater than 75°C (Etheridge, 2011).

Conventional techniques (e.g. laser doppler anemometry, LDA, or PIV) can be used to characterize the boundary conditions around buildings. Direct pressure measurements are less frequent, as characterizing pressure distributions with a high resolution on building surfaces can be challenging, especially when the pressure values are small (Nathan et al., 2021).

2.4.3. Recent advances and outlook

Simulating natural ventilation in a fluid tunnel has great potential, but also has several limitations, as explained above. Indoor and outdoor studies have traditionally been carried out independently, usually for different purposes, and only recently some research projects have started the connection between the two environments (see, for example, the MAGIC project by Song et al. (2018) in Fig. 5a). One of the major research gaps is the lack of studies on the impact of combined wind- and buoyancy-driven flows on the the interaction between indoor and outdoor environments, as remarks stated in Table A1 in the appendix. Better experimental techniques in both wind and water tunnels will allow a more complete characterization of natural ventilation in urban areas.

Thermal characterization of the building boundary conditions cannot be achieved easily in non-specialized facilities, but some specialized ones are starting to bridge the gap, with studies on non-neutral urban boundary layer (UBL) flows (Marucci and Carpentieri, 2020a; Marucci and Carpentieri, 2020b) and local heating sources (Marucci and Carpentieri, 2019; see Fig. 5b). Recent advances include the development of post-processing techniques for measuring the pressure fluctuations in low-speed wind tunnels where the variations are very small (Nathan et al., 2021). A better characterization of the building boundary will be crucial in developing reliable models for natural ventilation.

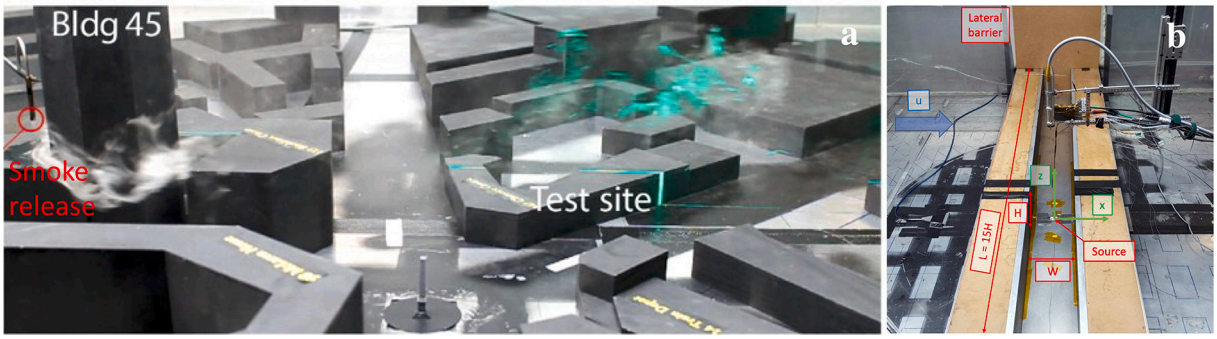

Fig. 5. (a) Study of combined wind- and buoyancy-driven ventilation (Song et al., 2018) and (b) study of the effects of local buoyancy sources on flow and dispersion in street canyons (Marucci and Carpentieri, 2019); both studies were from the EnFlo wind tunnel, University of Surrey, UK.

2.5. Modeling of vegetation

2.5.1. Fundamental considerations

Flow inside and past vegetation is complex. Vegetation elements such as leaves, needles, twigs, branches, and trunks span length scales from a few millimeters to tens of meters, hence comprise a range of four orders of magnitude. At their surfaces, boundary layers and wakes develop, which interact with each other and form shear layers and other intricate flow structures. The fundamental physical phenomena occurring in the flow through vegetation are (i) extraction of momentum due to aerodynamic resistance, (ii) conversion of mean into turbulence kinetic energy, and (iii) break-up of larger-scale turbulent motions into smaller-scale ones, and in this way, short-circuiting the eddy cascade (Shaw, 1985).

In reduced-scale fluid tunnel studies of the built and natural environments, the aerodynamic load and the modification of the flow and dispersion fields in the surrounding of vegetation are of interest (Fig. 6). Hence, scaling and similarity considerations should be directed on aerodynamic resistance (drag) and permeability. While scaling the aerodynamic resistance ensures similarity in the extraction of momentum from the flow, it does not ensure similarity in the kinematics of the flow. The latter requires scaling of the permeability, which implies the partitioning of the flow going through and around the vegetation. This is pivotal for the flow in the near wake, including the recirculation in the lee, and is particularly relevant in the built environment where the flow in the immediate vicinity of the vegetation is of interest, contrary to the natural environment where far wake characteristics or bulk quantities are of interest. The break-up of turbulent motions and short-circuiting of the eddy cascade are inherently complied with, however, only in a qualitative manner. A rigorous representation of all length scales, the short-circuiting of the eddy cascade, and all involved scales of turbulent motions elude scaling. This is because typical length scales and Reynolds numbers in reduced-scale experiments are two orders of magnitude smaller than the real scale.

2.5.2. Recommendations for the design of fluid tunnel experiments

To model vegetation in reduced-scale wind tunnel studies, it is recommended to utilize prefabricated plastic-based open porous foams. Such foams are commercially available from several manufacturers with various porosities denoted by PPI-x, where PPI stands for ‘pores per inch’ and x is their count. The foams are available for $7 < x < 100$ and can be processed to reproduce the contour of the vegetation under consideration (Fig. 6). Alternatively, open porous objects can be self-made as clusters of interwoven filament- or stripe-like components as successfully applied in previous works (Gromke and Ruck, 2008; Gromke and Ruck, 2009; Gromke, 2011; Li et al., 2022a)

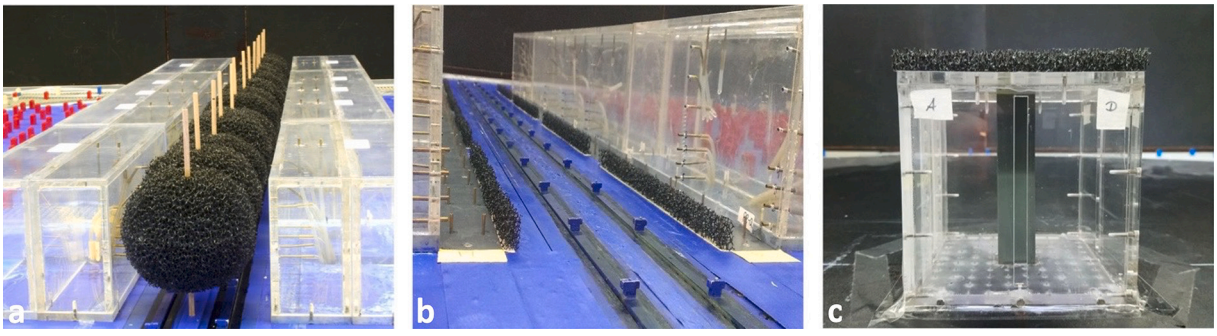

Fig. 6. Application examples of open porous foam processed to model (a) avenue-trees in an urban street canyon (Gromke and Ruck, 2007), (b) hedge-rows in a urban street canyon (Gromke et al., 2016), (c) roof greening of a building (Pappa et al., 2023).

To characterize the permeability for airflow of a porous medium in an aerodynamic manner, the pressure loss coefficient can be employed. The pressure loss coefficient λ of a porous sample in forced flow is defined as follows (Gromke, 2011):

$$\lambda = \frac{\Delta p_{st}}{p_{dyn}\, d} = \frac{p_{wwd} - p_{lwd}}{0.5\, \rho\, U^2\, d} \tag{2.5-1}$$

with Δp_{st} the difference in static pressure between windward (subscript ww) and leeward (subscript lwd) of the porous sample, p_{dyn} the dynamic pressure, ρ the fluid density, U the bulk flow speed, and d the porous sample thickness in streamwise direction. The λ-values of foams with identical PPI-value from various manufactures and production batches may vary to some extent. For example, $\lambda_{PPI\text{-}7} = 200$ m^{-1}, $\lambda_{PPI\text{-}10} = 250$ m^{-1}, $\lambda_{PPI\text{-}20} = 500$ m^{-1}, and $\lambda_{PPI\text{-}30} = 1000$ m^{-1}, which cover most of the required permeability of the model vegetation in fluid tunnel studies, can be adopted (Gromke et al., 2016; Klausmann and Ruck, 2017).

The similarity with regard to aerodynamic resistance is ensured if the ratio of momentum extraction F_{ed} by the (model) vegetation to the momentum of the undisturbed approach flow F_{af} is equal at the model scale and full scale, i.e., $[F_{ed}/F_{af}]_{ms} = [F_{ed}/F_{af}]_{fs}$, where subscripts ms and fs stand for model-scale and full-scale, respectively. As shown in Gromke (2011) and Gromke (2018), employing Eq. (2.5-1), the following relationship can be derived as:

$$\frac{\lambda_{fs}}{\lambda_{ms}} = \frac{d_{ms}}{d_{fs}} = M \tag{2.5-2}$$

where M denotes a geometric scale factor. Eq. (2.5-2) is the scaling relation that links the aerodynamic resistance, expressed by the pressure loss coefficient, of the model and real vegetation. The pressure loss coefficient of the model vegetation is that of the real vegetation divided by the geometric scale factor. For the pressure loss coefficients of real vegetation, the reader is referred to the study by Grunert et al. (1984). Herein, the pressure loss coefficients for various trees and shrub species in the normal foliated state are given as $1.8\ m^{-1} < \lambda_{fs} < 6.9\ m^{-1}$ at a wind speed of 4 ms^{-1} and as $0.8\ m^{-1} < \lambda_{fs} < 3.5\ m^{-1}$ at a wind speed of 11 ms^{-1}. Moreover, Table A1 in the appendix provides values for λ_{fs}.

The proposed scaling and similarity concept complies with the requirements for drag and permeability as outlined in the previous section on fundamental considerations. The modeling approach including the scaling and similarity concept is, next to its application in reduced-scale wind tunnel studies, applicable in investigations of scaled vegetation in water channels.

2.5.3. Recent advances and outlook

Recent fluid tunnel studies in urban environments have addressed the effects of greening on flow and turbulence, pollutant dispersion, and building ventilation. Gromke and Ruck (2012) and Fellini et al. (2022) revealed that dense rows of trees in urban street canyons (Fig. 6a) reduced their natural ventilation and resulted in higher concentrations of traffic pollutants. In contrast, street-flanking hedge rows (Fig. 6b) reduced the concentration of traffic pollutants in urban canyons (Gromke et al., 2016). The influence of roof or façade greening (Fig. 6c) on building ventilation and indoor air quality was addressed by Pappa et al. (2023) and was found to cause increases or decreases in the building air exchange rate depending on the location of the vegetation and openings in the building envelope. In a study of green walls, Li et al. (2022a) found reduced natural ventilation in urban street canyons in the presence of vegetation facades.

The vegetation modeling approach described in this contribution was successfully applied in studies of the effect of avenue-trees and hedge-rows on flow and pollutant dispersion in urban street canyons (Gromke, 2011; Gromke and Ruck, 2012; Gromke et al., 2016) as well as flow above forest canopies and wind loads on trees in forest stands (Gromke and Ruck, 2018). In addition to their contribution to fundamental knowledge, the data from these studies are widely used for the validation of numerical flow simulations by computational fluid dynamics (CFD). In particular, the modeling concept described herein is due to its parametrization straightforwardly applicable or implementable in CFD (e.g. Balczó et al., 2009; Buccolieri et al., 2009; Salim et al., 2011; Moonen et al., 2013; Gromke and Blocken, 2015; Jeanjean et al., 2015; Vranckx et al., 2015; Morakinyo and Lam, 2016; Merlier et al., 2018; Moayedi and Hassanzadeh, 2022; Zhu et al., 2022).

Future advancements in the modeling of vegetation in fluid tunnel studies may envisage fluid-structure interactions typically occurring at moderate and high flow speeds(Stacey et al., 1994; Hao et al., 2020). Moreover, most of the model vegetation models utilized in the past and current investigations do not, or only partly, reproduce reconfiguration and streamlining. The associated aerodynamic effects, such as changes in permeability and reduction in drag coefficient with increasing flow speed, are generally not sufficiently represented (Manickathan et al., 2018). Future fluid tunnel studies in the nexus of vegetation and urban climate may address the effects of façade or roof greening and parks or green spaces on urban flows with their implications for air quality (Ysebaert et al., 2021) , natural ventilation (Li et al., 2022a), and cooling (Manickathan et al., 2022; Zhao et al., 2023)

2.6. Modeling of pollutant dispersion

2.6.1. Fundamental considerations

Pollutant dispersion in urban areas is driven by local meteorological conditions and urban morphology. Furthermore, the multiplicity of pollutants and sources broadens the range of parameters that affect this phenomenon. The ability to control the different variables individually and isolate their effects is the main advantage of dispersion studies in fluid tunnel experiments. Similarity in laboratory models for pollutant dispersion in urban areas is ensured by means of geometric similarity (the aspect ratio H/W of a street canyon and the planar and frontal areas of a district, i.e., AI_{pa} and AI_{fa}) and the matching of the main dimensionless numbers for the

flow field: *Re*, *Pr*, and *Sc* numbers (Snyder, 1981; Meroney, 2004; Tominaga and Stathopoulos, 2016; Mei et al., 2023). When buoyancy effects inside a street canyon are modeled, a local *Ri* (or densimetric *Fr*) should also be considered (Marucci and Carpentieri, 2019; Fellini et al., 2020). Moreover, specific similarity criteria concerning pollutant emissions, should be matched, including the geometric similarity of the source, *Re*, and *Fr* at the emission location, and the density and speed ratios at the emission location (Pournazeri et al., 2012; Marro et al., 2014). These parameters are fundamental for simulating the release of non-neutrally buoyant plumes from elevated sources within the city. To reproduce vehicle exhaust, the buoyancy effects and emission speed are generally neglected, and the similarity is attained using a tracer with a density similar to that of the fluid. However, in this case, traffic-induced turbulence has non-negligible effects on pollutant dispersion, and the similarity criterion by Plate (1982) can be applied (Gromke and Ruck, 2007).

2.6.2. Recommendations for the design of fluid tunnel experiments

Besides the urban geometry, a key component of the experimental setup is the emitting sources, which is generally elevated or ground-level point sources reproduced via metallic tubes or line sources to simulate exhaust from vehicles. The latter is designed to minimize the vertical momentum and maximize lateral homogeneity (Meroney et al., 1996). Above the line source, traffic-induced turbulence can be mimicked using plates mounted on rotating bells (Kastner-Klein et al., 2001), as shown in Fig. 7a.

A mixture of hydrocarbon and air is generally injected to simulate neutrally buoyant emissions in wind tunnel experiments (Yee et al., 2006; Salizzoni et al., 2009; Perry et al., 2016). Point concentration measurements were performed using a Flame Ionization Detector (FID). Alternatively, sulfur hexafluoride can be used as a tracer gas (Yassin et al., 2005; Gromke and Ruck, 2007; Chavez et al., 2011), which can be collected and sent to the detector via a capillary tube or taken from measurement taps at building walls. Water vapor produced by an H_2O atomizer and measured by humidity sensors has also been used as a tracer for dispersion over urban areas (Mo and Liu, 2018).

Buoyant plume emissions (Fig. 7c) in wind tunnels are reproduced using light or heavy gases (He, CO_2) or heated air (Robins et al., 2001; Snyder, 2001; Kanda et al., 2006). In the first case, a tiny quantity of gas tracer detectable by an FID is generally added to the buoyant gas (Vidali et al., 2022). In the second case, measurements are performed using standard thermocouples (Marro et al., 2014). In addition to gaseous sources, experiments have been conducted in wind tunnels to investigate sand transport in urban and suburban areas, to evaluate the effects on low-rise buildings and infrastructures (Huang et al., 2023). These experiments involve specific and extensive similarity criteria for sand particles, which have only been partially addressed to date (Raffaele et al., 2021). Fluorescent dyes are released as passive tracers in water tunnels and the LIF technique allows for simultaneous multipoint concentration measurements (Yee et al., 2006; Wangsawijaya et al., 2022) (Fig. 7b). Buoyancy effects can be obtained by mixing tracer dyes with alcohol and water or by releasing saltwater (Pournazeri et al., 2012).

To evaluate the chronic pollution in urban areas, it is often sufficient to estimate the average pollutant concentration over time. To ensure a reliable prediction, the acquisition and averaging time must be longer than the typical time scale of vortical structures within the domain (Pavageau and Schatzmann, 1999; Garbero et al., 2010). Conversely, the assessment of hazards due to toxic or explosive pollutants, or the impact of odors, requires the analysis of concentration fluctuations (Cassiani et al., 2020) from which higher-order concentration statistics and probability density functions can be determined (Gailis and Hill, 2006; Yee et al., 2006; Klein et al., 2011). The velocity and concentration must be simultaneously measured to estimate turbulent mass fluxes, which are key to understanding pollutant exchange in complex geometries (Carpentieri et al., 2012; Marro et al., 2020).

2.6.3. Recent advances and outlook

In recent decades, physical modeling in fluid tunnels have brought great advances in understanding the mechanisms of dispersion in urban areas at different scales (Britter and Hanna, 2003; Xia et al., 2014; Zhang et al., 2020; Wang et al., 2021). For a group of sparse obstacles in the wake regime (Fig. 7d), the planar and frontal area densities of buildings were found to affect the dispersion process,

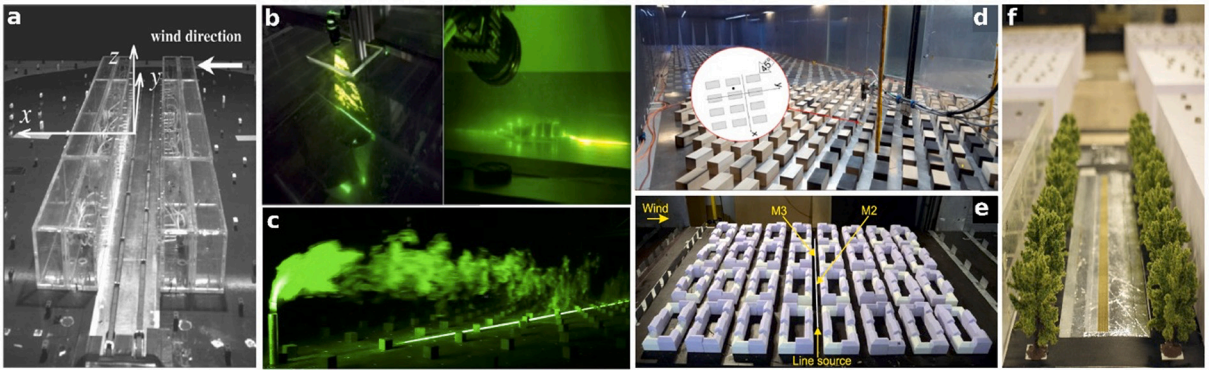

Fig. 7. Fluid tunnel testing of pollutant dispersion in cities: (a) moving belts along a street canyon to simulate two-lane traffic (Kastner-Klein et al., 2001). (b) PIV-PLIF setup in a water flume (Lim et al., 2022). (c) Laser tomographic visualization of heavy gas plume (Vidali, 2021). (d) Point source (Marucci and Carpentieri, 2020a) and (e) line source (Nosek et al., 2016) source at street level to simulate emissions in an urban array. (f) Street-level linear source mimicking pollutant dispersion in a vegetated canyon (Fellini et al., 2022).

and the concentration profiles within the building array were in good agreement with the Gaussian plume models (Davidson et al., 1996; Macdonald et al., 1998). This behavior differs between realistic and dense urban geometries (e.g. Garbero et al., 2010), where the decoupling between the layer above the roofs and the region within the streets leads to channelling effects, deflection of plume centreline and complex horizontal spreading. With regard to the effect of non-neutral approaching ABL winds on a regular array, the average concentrations in the canopy can be up to two times higher in stable stratification than in the neutral case and three times lower in convective conditions (Marucci and Carpentieri, 2020a). Much effort has been devoted to understanding dispersion in a single street canyon and at street intersections (Ahmad et al., 2005; Yazid et al., 2014). Recent research has shown that wall warming can lead to the deterioration or improvement of air quality, depending on the canyon aspect ratio (Marucci and Carpentieri, 2019; Fellini et al., 2020). Various studies (Hajra and Stathopoulos, 2012; Nosek et al., 2016; Llaguno-Munitxa et al., 2017) have shown that the shape of buildings and roofs (Fig. 7e) has a non-negligible effect on the concentration in the streets. Recently, there has been growing interest in the effects of tree planting (Fig. 7f) (Gromke and Ruck, 2007; Gromke and Ruck, 2009; Gromke and Ruck, 2012; Fellini et al., 2022) on pollutant dispersion in a single canyon.

To address the challenges related to climate change and urbanization, a greater number of experimental studies on the effects of vegetation, high spatial heterogeneity of buoyancy conditions, and deep and complex street canyons on air pollution are crucial, as highlighted and commented in Table A1 in the appendix. This review also reveals the lack of experimental data on the concentration of reactive plumes in urban geometries, which would be fundamental to validating the large number of numerical models covering the topic.

2.7. Modeling of outdoor wind thermal comfort

2.7.1. Fundamental considerations

Thermal comfort is a subjective evaluation of the thermal environment. Over the last century, researchers have created several thermal comfort models to predict human thermal responses to different combinations of environmental parameters (including air temperature, humidity, radiation, and wind velocity) and personal variables (e.g. clothing and activity levels) (Gagge et al., 1972; Fiala et al., 2012). The core of the performance of thermal comfort models is a realistic prediction of the impact of ground-level wind. The convective and evaporative heat loss from the human body to the surrounding environment are determined by the convective heat transfer coefficient (CHTC).

To measure anatomically specific CHTCs for individual body segments, thermal manikin experiments were conducted in fluid tunnels, which have the ability to generate a wide range of wind conditions in a limited time and to maintain the same wind conditions for a manikin to reach a steady state. The thermal manikin features an anatomically realistic human morphology, with a precision heating element and temperature sensor system embedded within the “skin”. It automatically measures the sensible heat transfer between the human body surface and surrounding environment by recording the electrical power input to each body segment (Tanabe et al., 1994; De Dear et al., 1997).

Forced convection over a human body can be characterized by the Prandtl number (Pr) along with the human-scale-based Reynolds number, as expressed in Eq. (2.7-1)

$$Re_{\mathrm{hs}} = U_{\mathrm{pdl}} CD_{\mathrm{hs}} / \upsilon \tag{2.7-1}$$

where U_{pdl} is the wind speed at the pedestrian level (m/s), CD_{hs} is the characteristic dimension of the body or segment (m), and ν is kinematic viscosity (m/s^2). It is worth noting that in wind tunnel measurements the wind speed at an equivalent pedestrian level should be used, while an “equivalent steady wind velocity” can be adopted to account for the effect of turbulence intensity (Hunt et al., 1976).

As the variation in *Pr* is marginal for air temperature ranging from 10 to 30 ^{o}C, the general form of CHTC describes the dependence on air speed, which can be written as Eq. (2.7-2) with m and n being regression coefficients for individual body segments.

$$\mathrm{CHTC} = \mathrm{m}U^{\mathrm{n}} \tag{2.7-2}$$

2.7.2. Recommendations for the design of fluid tunnel experiments

In general, velocity is required to characterize the incoming flow; however, for turbulent flow, the turbulence intensity and turbulence length scale are also required. Therefore, pedestrian-level turbulence characteristics must be properly simulated for thermal comfort studies in fluid tunnel modeling (Zhou et al., 2006). Turbulence generators, such as oscillating aerofoils and passive grids (Fig. 8b), were implemented upstream to simulate full-scale natural wind. The approaching wind profile or wind profile close to the body segments must be measured using fast-response anemometers.

The manikin is often placed at the center of the fluid tunnel test section in a sitting, standing, or walking posture (Fig. 8a-c), and tested under target wind conditions. The CHTC is calculated based on the thermal state (skin temperature and heat loss) automatically logged by the manikin itself, and the air temperature and wind tunnel inner surface temperature can be measured by additional temperature sensors (Fig. 8a). The relationship between the CHTC and approaching wind conditions is generally established through empirical regressions.

To further investigate the physiological and perceptual responses of pedestrians to wind, human subjects were invited to the wind tunnel to experience different wind conditions. Their thermal physiological parameters (e.g. local skin temperature) and perceptual responses can be collected and compared with the thermal comfort model output (Yu et al., 2021).

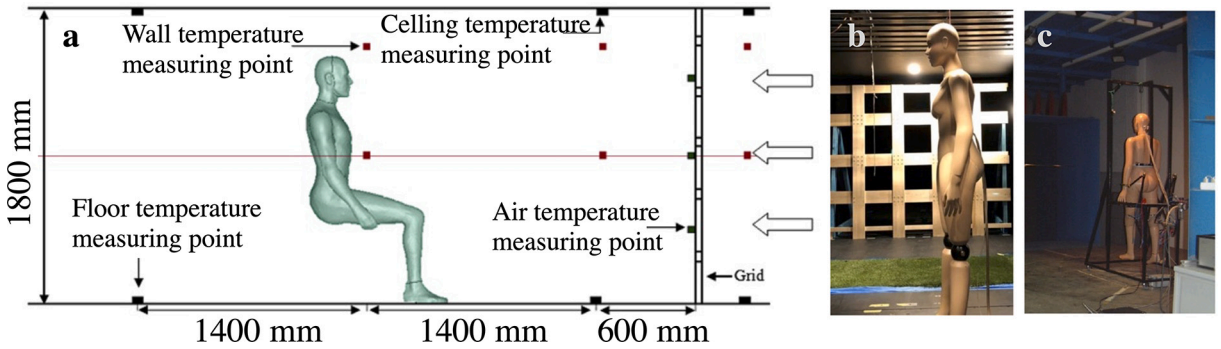

Fig. 8. Wind tunnel testing on convective heat transfer coefficient: (a) a schematic diagram of the wind tunnel setup and a thermal manikin in a sitting posture, modified from Li and Ito (2014); (b) a thermal manikin in a standing posture downwind of a passive turbulence generator (Yu et al., 2020); and (c) a thermal manikin in a walking posture, modified from Oliveira et al. (2014).

2.7.3. Recent advances and outlook

Thermal manikin and human subject experiments in fluid tunnels have enabled us to quantify the impact of wind on thermal perception. The CHTCs for individual body segments and the whole-body are generated for typical outdoor wind conditions, including wind speed from still air to approximately 13 m s^{-1} (Li and Ito, 2014), turbulence intensity from 0 to approximately 30% (Yu et al., 2020), evenly spaced horizontal directions, and different body postures, including sitting, standing, and walking. The prevailing thermal comfort models should adjust the CHTC formula according to the target environment and activity conditions to improve the prediction accuracy.

While the effects of wind on sensible heat loss have been thoroughly investigated in the literature, few studies have focused on evaporative heat loss, which plays a role in determining thermal comfort when sweat accumulation increases (Bakkevig and Nielsen, 1995). To better understand the impact of body motion on CHTCs, the flow field around manikins or human subjects during activities such as walking and cycling is worthy of further investigation (Luo et al., 2014).

Based on field measurements in urban areas, pedestrian-level turbulence intensity ranging between 10% and 60% is not uncommon (Murakami and Deguchi, 1981; Tse et al., 2017; Zou et al., 2021), and approximately half of the energy of the turbulence concentrates at frequencies less than 0.1 Hz (Hunt et al., 1976). More work is required to reproduce a full-scale wind profile in a fluid tunnel with high turbulence intensity and low-frequency random gustiness. Differentiating the role of turbulence length scale from turbulence intensity will allow a more accurate approach for predicting convective heat loss in real urban environments. A remark on this particular aspect is given in Table A1 in the appendix. Future research efforts could also be applied to the interaction effect between wind and radiation by introducing solar simulators into fluid tunnels.

2.8. Modeling of wind flows over complex urban sites

2.8.1. Fundamental considerations

The use of fluid tunnels to test wind flows at complex urban sites or a small portion of these sites has a long heritage. Probably the first experiments inspecting the effect of adjacent buildings were carried out by Harris in 1934 on the Empire State Building (New York, USA) at the wind tunnel facility of the Bureau of Standards (Harris, 1934). Since then, an increasing number of studies have been conducted, not only on isolated buildings/structures but also on realistic urban models (e.g. Mo and Liu, 2023), leading to a significant improvement in wind tunnel facilities, measurement techniques, and the overall scientific background (Fig. 9).

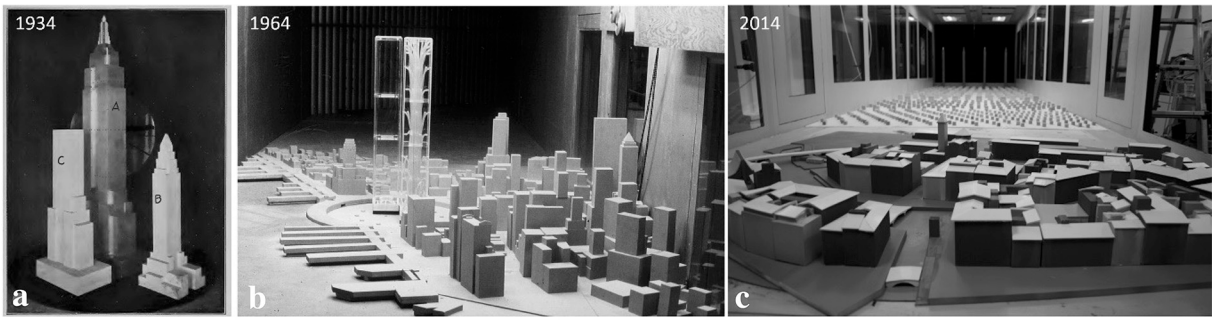

Fig. 9. Wind tunnel testing of parts of realistic urban districts or cities: (*a*) Empire State Building and its immediate surroundings, USA, modified from (Harris, 1934); (*b*) Twin Towers of the New York Trade Center, USA, modified from Plate (1999); (*c*) district of Quartiere La Venezia, Livorno city, Italy.

In 2022, despite the different eras and progress made in numerical simulations and field measurements over different decades, the use of fluid tunnels for testing realistic, complex urban sites remains remarkably high. This is justified by the fact that academics and practitioners typically find practical and reliable solutions for a large variety of topics in urban physics (e.g. Moonen et al., 2012) and wind engineering (e.g.Blocken, 2014; Solari, 2019; Kareem, 2020; H'ng et al., 2022), such as the high pollutant dispersion (e.g. Li et al., 2021b; Nosek et al., 2021), pedestrian-level wind discomfort (Blocken et al., 2016; Gaber et al., 2020; Gao et al., 2022), indoor/outdoor thermal comfort (e.g. Stathopoulos et al., 2004), wind energy (Joselin Herbert et al., 2007; Stathopoulos et al., 2018), wind loading (Davenport, 2002; Simiu and Yeo, 2019), and influence of severe convective gusts (Richter et al., 2018).

As mentioned earlier, proper downscaling of atmospheric winds and realistic urban models is generally quite challenging. Publications released in the last 50 years have not only further enhanced the scientific background previously developed, but have also provided useful practical guidelines for accurately reproducing scaled neutral, stable, and unstable atmospheric boundary layer (ABL) winds (Stull, 1988) in fluid tunnel tests (ASCE/SEI 49-12, 2012). Important aspects related to the similarity criteria (geometric, kinematic, and dynamic) to be satisfied between full and reduced scales, both for the ABL flow and urban model, have been extensively investigated. On this basis, a large variety of setups of roughness fetch and vortex generators (i.e. spires) to accurately reproduce the turbulent structures of the approach ABL flow in an empty test section or upstream of scaled models have been systematically calibrated and tested in aeronautical, climatic, and ABL fluid tunnels. In particular, a set of key parameters have been extensively monitored and found to be crucial for the proper development of a neutral ABL wind along the wind tunnel test section: mean velocity profiles, streamwise turbulence intensity, lateral turbulence intensity, vertical turbulence intensity, power spectral density distributions, and integral length scales of turbulence (Cermak, 1975). However, the agreement between reduced-scale experimental data and meteorological data from codes and standards remains an important topic to be addressed to guarantee the validity of scaled wind characteristics.

2.8.2. Recommendations for the design of fluid tunnel experiments

Matching the most relevant dimensionless parameters between the reduced scale and full scale can almost never be fully realized. There is almost a general consensus that the exact matching of some of these parameters might not be that relevant for urban flow studies. In most cases, the buildings of realistic urban models are characterized by sharp edges with fixed separation points of the flow, leading to the overall assumption of *Re*-independency. However, as stressed by Baker (2007) "*it would be wise to give further consideration to the commonplace assumption that Reynolds number effects can be neglected provided a minimum value is achieved in wind tunnel tests*". Indications on the match of *Re* number in complex urban sites are currently lacking in the scientific literature, but results obtained from specific investigations on bluff bodies (e.g. Bai and Alam, 2018), isolated buildings (e.g. Khaled and Aly, 2022), on street canyons (e.g. Lin et al., 2021) and idealized urban models (e.g. Shu et al., 2020) can be still used to better understand phenomena in complex environments. The equality of the Jensen number (*Je*) (Holmes and Carpenter, 1990), such as the ratio of the building height to aerodynamic roughness length (z_0), is also important for the similarity of buildings immersed in ABL flows. In the case of realistic urban sites, a match of this number could be achieved upstream of the explicitly modeled urban site, as for an isolated building at the end of the roughness fetch, but not in its middle. The *Ri*, *Gr* and *Sc* may play a key role in properly scaling thermal effects and dispersion phenomena, as stressed in previous sections.

In addition, there are other important aspects that may be crucial for the choice of the geometric scale factor (*M*): (i) the fluid tunnel test-section length to properly develop the approach ABL (Cermak, 1975); (ii) the blockage ratio being less than 5% (e.g. see ASCE/SEI 49-12, 2012); (iii) the need to manufacture small-scale architectural features to avoid oversimplifications that might threaten the reliability of the experimental results (e.g. Carpentieri and Robins, 2015; Ricci et al., 2017b; Pađen et al., 2022); and (iv) the encompassing a sufficient portion of the environment surrounding the area of interest (Ricci et al., 2022). Hence, it is clear that defying the most appropriate scale of a realistic urban model is ultimately a compromise of multiple factors, which gives rise to a wide range of commonly adopted scales, from 1:100 (for small districts) to 1:2000 (for large portions of cities). With such small scales, the choice of materials and manufacturing techniques can also help improve the resolution of geometries by significantly reducing the gap between reality and models. Geometrical simplifications adopted for buildings or a portion of these might have an influence on the UBL and urban canopy layer (UCL) development but also on the local wind flow pattern (e.g. inside canyon streets) (Ricci et al., 2017a; Ricci et al., 2017b).

The choice of materials is also strictly related to the type of tests to be performed (e.g. wind speed, wind pressure, temperature, and pollutant dispersion measurements) and, consequently, to the instrumentation that should be used (e.g. pressure taps, Irwin probes, cobra probe, hot-wire anemometry, laser-Doppler anemometry, PIV). From this perspective, due to the small dimensions of buildings and streets, the use of a nonintrusive and accurate measurement technique is highly recommended for urban models. The advantages and disadvantages of measurement techniques can differ when related to specific topics; however, providing an exhaustive overview is beyond the scope of this paper. Finally, because these models often extend beyond the fluid tunnel turntable, it is equally important to accurately define the monitored area of the models (where measurements will be performed), preferably far away from the lateral boundaries of the facility, by avoiding any possible undesirable interference effects (Stathopoulos and Surry, 1983).

2.8.3. Recent advances and outlook

Most advanced techniques, such as 3D printing and injection moulding, can facilitate the manufacture of complex, realistic urban models, improve the geometry resolution, and pre-arrange during the design stage of the model for sensor installation (e.g. pressure taps) to definitively reduce the discrepancies between reality and models. In this regard, numerical techniques (e.g. CFD), as a complementary tool to support the fluid tunnel tests of ABL winds in realistic urban models, might help to gain a better understanding of (i) the size of the surrounding environment to be realized for fluid tunnel tests, (ii) the level of geometrical simplifications to be adopted for buildings and other urban features, and (iii) the UBL and UCL development through and over the investigated area.

Nevertheless, climate change and the increasing number of extreme events, unlike most ordinary ABL winds, are boosting efforts to detect, test, simulate, and model thunderstorm outflows and tornadoes worldwide (Hangan et al., 2017; Solari et al., 2020). The use of new fluid tunnel typologies and dedicated tornado/downburst simulators that can host extensive urban models has become a reality. However, due to downscaling and similarity issues (e.g. defining the most appropriate geometrical scale factor), most studies have focused on empty chambers or isolated structures/buildings. This trend is bound to change, and most likely, more experimental tests on realistic urban models (e.g. $M > 1{:}2000$) and realistic thermal conditions will be carried out in the near future to make buildings and cities more resilient, which are important future studies as highlighted in Table A1 in the appendix.

In conclusion, if on one hand the main findings of realistic urban studies are difficult to generalize and be used for basic analytical formulations (as for idealized case studies), on the other hand it has to be acknowledged that probably this is one of the best "trade-off" between academicians and practitioners to gain a reliable understanding of the wind flow field around buildings amidst well-settled urban layouts and provide feasible solutions to actual problems.

3. Three challenges for fluid tunnel modeling of the urban climate

3.1. Modeling of multiphysics

Multiphysics processes occur in cities where people live, and they include the absorption of solar radiation and the emission of heat from urban materials, convective heat transport by wind, evapotranspiration of plants, evaporation of water bodies, release of anthropogenic heat, emission and dispersion of pollutants, and others. Physical modeling of these processes in fluid tunnels is extremely challenging, if not impossible. The challenges lie in (i) deriving scaling among the multiphysics processes, (ii) complex setups for generating these phenomena simultaneously, and (iii) limited capabilities for large-scale flow, temperature, and humidity measurements.

Scaling has been well established for isothermal airflow studies using fluid tunnels in which Reynolds-number-independency often is assumed (e.g. Chew et al., 2018; Shu et al., 2020), although, as mentioned in Section 2.8, it is always highly recommended to conduct specific tests for this purpose. For buoyancy-involved or non-isothermal airflow, the Richardson number has been accepted as the proper characteristic dimensionless parameter (Aliabadi et al., 2019; Zhao et al., 2022b). However, there are few well-established scaling criteria for other physical processes. As an example, scaling for urban surface heat budget that is dominated by shortwave and longwave radiation, convective heat transfer, and heat storage by urban materials, has not been established for scaled-down experimental studies. Present studies of these physical processes usually prescribe constant surface temperature or heating capacity to mimic urban heat to some extent. Shading and transpirative cooling by vegetation and plants in urban areas, as another example, could be studied using fluid tunnel experiments based on thoughtful scaling analysis (Manickathan et al., 2022).

In addition, complex experimental setups are needed to reproduce multiphysics processes in a fluid tunnel. Experimental setups in the field of urban climate often are designed to study a particular physical process, rather than to study coupled multiple processes. For studies of urban isothermal wind, fluid tunnel measurements based on scaled-down realistic neighbourhood models have been the norm. This could be the basis upon which other physical processes, such as the heterogeneous urban surface heat budget, could be realized by introducing artificial solar radiation and thoughtfully selecting the materials used for buildings to mimic the absorption and emission of heat. In addition, the cooling effects of living vegetation alongside complex urban streets may be physically modelled using small-sized potted plants.

Substantial developments of both measurement techniques and advanced post-processing abilities are still much needed for fluid tunnel studies of the urban climate. For isothermal airflow, planar- and stereo-PIV have been developed to an advanced level that allows accurate velocity fields to be obtained. The recent development of the water tunnel (flume) PIV-LIF measurement technique provides a way to obtain velocity and temperature fields simultaneously and thus to better understand turbulent and convective heat transport processes (Zhao et al., 2022b). However, for the modeling of winds in wind tunnels, the measurements of field measurements still rely mainly on individual thermocouple measurements at certain locations. Instruments that allow the measurement of air temperature and humidity measurements for a large FOV need to be developed for studies modeling coupled heat and moisture transport in complex urban sites. The development of these instruments should take mobility and flexibility into account to allow efficient measurements with multiple FOVs.

3.2. Modeling of anthropogenic processes

Urban climates involve complex interplay of many anthropogenic processes and synoptic climate (Kubilay et al., 2020; Masson et al., 2020). These typical processes include, but are not limited to, the emission of anthropogenic heat through air-conditioners, transportation, and industrial plants (Mei and Yuan, 2021). The emission of pollutants in the form of aerosols may particularly affect the radiation in the lower atmosphere and even the formation of clouds and precipitation (Masson, 2006; Nazarian et al., 2018). To reproduce urban climate phenomena in fluid tunnels, stochastic and anthropogenic processes in different forms must be taken into account.

The challenges to reproducing anthropogenic processes in the urban climate in fluid tunnels lie primarily in the mimicking of spatial- and temporal-inhomogeneous heat and pollutant sources. As an example, on one hand, to simulate the impacts of spatially inhomogeneous release of anthropogenic heat in different residential areas, accurately designed heating elements in a fluid tunnel are

required. These elements should be capable of maintaining the desired spatially-varied surface temperatures. In addition, the controllable heating elements should be able to reproduce and mimic the temporal variation of the release of anthropogenic heat, such as varying the operational capacity of Heating, Ventilation, and Air Conditioning (HVAC) systems due to different cooling demands during the day. As another example, to study inhomogeneous air quality in cities or in a neighbourhood, spatially-dependent and temporally- dependent anthropogenic pollutant emission processes should be modelled in fluid tunnels.

How to couple these anthropogenic, stochastic processes to prevailing wind, heat, and moisture transport processes at realistic spatial and temporal scales remains another key challenge for fluid tunnel modeling. It has been well established to model meteorological conditions (e.g. wind) from the statistical point of view of prevailing characteristics. However, when it comes to highly time-dependent or fast evolving anthropogenic processes, multiple time scales have to be considered and realized in fluid tunnel modeling to both characterize the prevailing (background) urban climate and timewise (superimposed) characteristics.

Given the complexity in matching various spatiotemporal scales, not to mention the development of case-specific experimental setups, the best use of fluid tunnel modeling to understand stochastic anthropogenic processes may lie in providing benchmark experimental modeling data for validation and calibration of CFD models, which ultimately facilitates numerical studies of the full-scale urban climate. High-quality experimental data from fluid tunnels on anthropogenic heat or pollutant emission processes involving varying intensities of wind flow turbulence and buoyancy are much needed for CFD model development, in particular for modeling turbulence and determining the correct treatment of the buoyancy term.

3.3. Combined fluid tunnel, scaled outdoor and field measurements

While full-scale field experiments ($H \sim 10$ - 100 m) provide a reliable way to understand the urban climate (Eliasson et al., 2006; Offerle et al., 2007), diurnal cycles of urban thermal environment, including solar radiation, thermal storage by urban materials, vegetation transpiration and others, are difficult to model in fluid tunnels. Furthermore, urban geometric layouts and building surface materials in cities are highly heterogeneous, and thermal boundaries are complicated and usually difficult to quantify.

Scaled outdoor measurements ($H \sim 1$ m) have been verified as a good option to obtain high-quality parametric experimental data under realistic meteorological conditions (e.g. Yee and Biltoft, 2004; Kawai and Kanda, 2010; Chen et al., 2020). One of the paramount advantages of scaled outdoor measurements is the representation of physical processes that may rely on nature and various realistic conditions, such as solar radiation. Also, scaled outdoor measurements usually allow models one order of magnitude larger compared to fluid tunnel models, which facilitates the matching of characteristic dimensionless numbers. As an example, compared to fluid tunnel studies in which scaled-down models are in the range of $H \sim 0.1$ m, scaled outdoor models are in the range of $H \sim 1$ m. Building models of complex geometries or living vegetation of different species (e.g. trees and shrubs) may be realized in-situ at the measurement site without the need for an additional setup.

Since it is difficult or even impossible to satisfy all similarity requirements for scaled experimental studies either in laboratory or in an outdoor setting, a promising and viable approach for investigating urban airflow and the thermal environment may be to rely on the combination of numerical simulations and experiments at various scales, i.e., full-scale field measurements, scaled outdoor measurements and fluid tunnel experiments. Conducting measurements covering this wide range of scales also allows us to develop a better understanding of the effects of scaling and to identify physical processes that are particularly sensitive to scaling.

4. Concluding remarks

In this paper, the capabilities of fluid (wind and water) tunnels for modeling the effect of the urban climate on eight important physical processes were reviewed. These physical processes involve solar radiation, inhomogeneous thermal buoyancy effects, thermal stratification, indoor and outdoor ventilation, aerodynamic effects of vegetation, dispersion of pollutants, outdoor wind thermal comfort and wind dynamics in complex urban settings. Fundamental considerations, recommendations for design of experimental modeling, recent advances, and an utlook were provided for each topic, and they serve as a repository of the state-of-the-art of physical modeling using fluid tunnels. A summary of key parameters of interest for each topic also is provided in Table A1 in the Appendix.

While substantial advances have been made in the modeling of decoupled, individual physical processes, grand challenges lie ahead in (i) physical modeling of coupled physical processes, (ii) mimicking of stochastic anthropogenic heat and pollution processes, and (iii) scaling of the different multiphysics processes. Fluid tunnel modeling of the multiphysics processes that dominate the urban climate, such as the joint effects of evapotranspiration of plants and wind flow in complex and realistic urban morphology, is much needed in order to understand the physics and also for the validation of the advanced numerical models that solve the multiphysics problems of the urban climate. In addition to the challenges in realizing those physical processes in fluid tunnels, establishing proper scaling for scaled-down multiphysics processes and full-scale scenarios is even more challenging, and additional research efforts are needed, particularly those associated with theoretical analyses.

To tackle these great challenges, a research consortium that comprises experienced researchers working on different urban climate processes is imperative. The rich expertise of such a research consortium would facilitate the design of advanced experimental setups for generating and studying a combination or full set of those important physical processes. The realization and outcome of fluid tunnel modeling of multiphysics urban processes would in parallel contribute to validation and enhancement of advanced numerical models for urban climate studies.

CRediT authorship contribution statement

Yongling Zhao: Conceptualization, Writing – original draft, Writing – review & editing. **Lup Wai Chew:** Writing – original draft, Writing – review & editing. **Yifan Fan:** Writing – original draft, Writing – review & editing. **Christof Gromke:** Writing – original draft, Writing – review & editing. **Jian Hang:** Writing – original draft, Writing – review & editing. **Yichen Yu:** Writing – original draft, Writing – review & editing. **Alessio Ricci:** Writing – original draft, Writing – review & editing. **Yan Zhang:** Writing – original draft, Writing – review & editing. **Yunpeng Xue:** Writing – original draft, Writing – review & editing. **Sofia Fellini:** Writing – original draft, Writing – review & editing. **Parham A. Mirzaei:** Writing – original draft, Writing – review & editing. **Naiping Gao:** Writing – original draft, Writing – review & editing. **Matteo Carpentieri:** Writing – original draft, Writing – review & editing. **Pietro Salizzoni:** Writing – review & editing. **Jianlei Niu:** Writing – review & editing. **Jan Carmeliet:** Writing – review & editing.

Declaration of Competing Interest

The authors declare that they have no known competing financial interests or personal relationships that could have appeared to influence the work reported in this paper.

Data availability

Data will be made available on request.

Acknowledgements

Y. Zhao, Y. Xue and J. Carmeliet acknowledge the funding support from the Swiss National Science Foundation (Grant 200021 169323). Y. Fan acknowledges the Fundamental Research Funds for the Central Universities (K20220163). Y. Zhao is also grateful for the guest researcher position at EMPA (Swiss Federal Laboratories for Materials Science and Technology) where some of the experimental studies were conducted.

Appendix A

Table A1
Parameters of interests and remarks on the eight topics for future studies.

Topics	Parameters for future studies	Remarks
Solar radiation	• $G < 400$ W/m^2 • $Re < 5 \times 10^6$ • $0 < \varepsilon < 1$	• A full range of shortwave radiation intensity (G) can be explored. • A wide range of wind speed (characterized by Re) needs to be reproduced in measurements. • The impact of building materials of various emissivity (ε) on radiative and convective heat transfer should be studied systematically.
Inhomogeneous thermal buoyancy effects	• $Ri_b > 4.4$ • $H/W \gg 2.3$ • $\psi \gg 2.5$	• Stronger buoyancy representing extreme hot weather is worthy of studies. • Natural ventilation in narrow street canyons is worse and thus deserve more research. • Realistic street canyon configurations, for instance the steepness ratio ψ, need to be explored.
Thermal stratification	• $0.01 < Fr < 0.03$ • $R_0 < 3$	• The urban heat dome flow over a large city is characterized by the large urban diameter (10-40 km) and small mixing height (0.5-1.5 km). • Coriolis force is particularly important for cities with large latitude and urban diameter.
Indoor and outdoor natural ventilation	• Re • Pe • Indoor/outdoor morphology	• Buoyancy-driven flows need to be studied in combination with wind-driven flows. • The effect of the surrounding environment on the indoor/outdoor exchange needs to be better understood
Vegetation	• $0.2 \leq \lambda_{fs} \leq 13$	• The lower range corresponds to vegetation with only few leaves or leafless vegetation (e.g. in winter). • The upper range corresponds to very dense vegetation as found in vegetation shelterbelts consisting of intertwined trees and shrubs or in very dense hedges.
Pollutant dispersion	• $H/W \gg 2$ • Ri (time and spatial dependent)	• Pollutant dispersion in deep street canyons. • Pollutant dispersion subject to complex spatial and temporal buoyancy conditions
Outdoor wind thermal comfort	• $TI > 30\%$ • ξ (turbulence length scale)	• Pedestrian-level wind in urban environments features a high turbulence intensity, and there exist a wide range of eddy sizes. • The effect of turbulence length scale on human body convective heat transfer coefficient hasn't been studied.
Urban flow over complex urban sites	• T to be considered • $M >$ 1:2000	• Fluid tunnel studies on realistic urban sites accounting for thermal effects are rare in the scientific literature. • Few fluid tunnels worldwide are capable to accommodate large realistic urban models with high-resolution architectural features.

References

Ahmad, K., Khare, M., Chaudhry, K., 2005. Wind tunnel simulation studies on dispersion at urban street canyons and intersections—a review. J. Wind Eng. Ind. Aerodyn. 93 (9), 697–717.

Aliabadi, A.A., Moradi, M., Clement, D., Lubitz, W.D., Gharabaghi, B., 2019. Flow and temperature dynamics in an urban canyon under a comprehensive set of wind directions, wind speeds, and thermal stability conditions. Environ. Fluid Mech. 19 (1), 81–109. https://doi.org/10.1007/s10652-018-9606-8.

Allegrini, J., Dorer, V., Carmeliet, J., 2013. Wind tunnel measurements of buoyant flows in street canyons. Build. Environ. 59, 315–326.

Allegrini, J., Dorer, V., Carmeliet, J., 2014. Buoyant flows in street canyons: validation of CFD simulations with wind tunnel measurements. Build. Environ. 72, 63–74. https://doi.org/10.1016/j.buildenv.2013.10.021.

ASCE/SEI 49-12, 2012. Wind Tunnel Testing for Buildings and Other Structures. Am. Soc. Civil Eng. ISBN(PDF).

Bai, H., Alam, M.M., 2018. Dependence of square cylinder wake on Reynolds number. Phys. Fluids 30 (1), 015102. https://doi.org/10.1063/1.4996945.

Baker, C., 2007. Wind engineering—Past, present and future. J. Wind Eng. Ind. Aerodyn. 95 (9-11), 843–870.

Bakkevig, M.K., Nielsen, R., 1995. The impact of activity level on sweat accumulation and thermal comfort using different underwear. Ergonomics 38 (5), 926–939.

Balczó, M., Gromke, C., Ruck, B., 2009. Numerical modeling of flow and pollutant dispersion in street canyons with tree planting. Meteorol. Z. 18 (2), 197–206. https://doi.org/10.1127/0941-2948/2009/0361.

Blocken, B., 2014. 50 years of computational wind engineering: past, present and future. J. Wind Eng. Ind. Aerodyn. 129, 69–102.

Blocken, B., Gualtieri, C., 2012. Ten iterative steps for model development and evaluation applied to computational fluid dynamics for environmental fluid mechanics. Environ. Model Softw. 33, 1–22. https://doi.org/10.1016/j.envsoft.2012.02.001.

Blocken, B., Stathopoulos, T., van Beeck, J.P.A.J., 2016. Pedestrian-level wind conditions around buildings: review of wind-tunnel and CFD techniques and their accuracy for wind comfort assessment. Build. Environ. 100, 50–81. https://doi.org/10.1016/j.buildenv.2016.02.004.

Britter, R., Hanna, S., 2003. Flow and dispersion in urban areas. Annu. Rev. Fluid Mech. 35 (1), 469–496.

Britter, R., Schatzmann, M., 2010. COST 732: The Model Evaluation Guidance and Protocol Document.

Buccolieri, R., Gromke, C., Di Sabatino, S., Ruck, B., 2009. Aerodynamic effects of trees on pollutant concentration in street canyons. Sci. Total Environ. 407 (19), 5247–5256. https://doi.org/10.1016/j.scitotenv.2009.06.016.

Carpentieri, M., Robins, A.G., 2015. Influence of urban morphology on air flow over building arrays. J. Wind Eng. Ind. Aerodyn. 145, 61–74.

Carpentieri, M., Hayden, P., Robins, A.G., 2012. Wind tunnel measurements of pollutant turbulent fluxes in urban intersections. Atmos. Environ. 46, 669–674.

Cassiani, M., Bertagni, M.B., Marro, M., Salizzoni, P., 2020. Concentration fluctuations from localized atmospheric releases. Bound.-Layer Meteorol. 177 (2), 461–510.

Castro, I., Robins, A., 1977. The flow around a surface-mounted cube in uniform and turbulent streams. J. Fluid Mech. 79 (2), 307–335.

Catarelli, R.A., Fernández-Cabán, P.L., Masters, F.J., Bridge, J.A., Gurley, K.R., Matyas, C.J., 2020. Automated terrain generation for precise atmospheric boundary layer simulation in the wind tunnel. J. Wind Eng. Ind. Aerodyn. 207, 104276 https://doi.org/10.1016/j.jweia.2020.104276.

Cenedese, A., Monti, P., 2003. Interaction between an inland urban heat island and a sea-breeze flow: a laboratory study. J. Appl. Meteorol. Climatol. 42 (11), 1569–1583.

Cermak, J.E., 1975. Applications of Fluid Mechanics to Wind Engineering—A Freeman Scholar Lecture.

Chang, Y.-S., Chen, Y.-J., Qiu, Y.-H., Chien, C.C., Chu, C.-C., Lee, F.-S., 2021. Source-like patterns of flow past a circular cylinder of finite span at low Reynolds numbers. Phys. Fluids 33 (8), 083607. https://doi.org/10.1063/5.0056885.

Chavez, M., Hajra, B., Stathopoulos, T., Bahloul, A., 2011. Near-field pollutant dispersion in the built environment by CFD and wind tunnel simulations. J. Wind Eng. Ind. Aerodyn. 99 (4), 330–339.

Chen, G., Yang, X., Yang, H., Hang, J., Lin, Y., Wang, X., Wang, Q., Liu, Y., 2020. The influence of aspect ratios and solar heating on flow and ventilation in 2D street canyons by scaled outdoor experiments. Build. Environ. 185, 107159.

Chew, L.W., Nazarian, N., Norford, L., 2017. Pedestrian-level urban wind flow enhancement with wind catchers. Atmosphere 8 (9), 159.

Chew, L.W., Aliabadi, A.A., Norford, L.K., 2018. Flows across high aspect ratio street canyons: Reynolds number independence revisited. Environ. Fluid Mech. 18 (5), 1275–1291.

Clements, C.B., Whiteman, C.D., Horel, J.D., 2003. Cold-air-pool structure and evolution in a mountain basin: Peter Sinks, Utah. J. Appl. Meteorol. 42 (6), 752–768.

Cui, P.-Y., Li, Z., Tao, W.-Q., 2016. Wind-tunnel measurements for thermal effects on the air flow and pollutant dispersion through different scale urban areas. Build. Environ. 97, 137–151.

Czarnecka, M., Nidzgorska-Lencewicz, J., 2017. The impact of thermal inversion on the variability of PM10 concentration in winter seasons in Tricity. Environ. Prot. Eng. 43 (2).

Dallman, A., Magnusson, S., Britter, R., Norford, L., Entekhabi, D., Fernando, H.J.S., 2014. Conditions for thermal circulation in urban street canyons. Build. Environ. 80, 184–191. https://doi.org/10.1016/j.buildenv.2014.05.014.

Davenport, A.G., 2002. Past, present and future of wind engineering. J. Wind Eng. Ind. Aerodyn. 90 (12–15), 1371–1380.

Davidson, M., Snyder, W., Lawson Jr., R., Hunt, J., 1996. Wind tunnel simulations of plume dispersion through groups of obstacles. Atmos. Environ. 30 (22), 3715–3731.

Davies Wykes, M.S., Chahour, E., Linden, P.F., 2020. The effect of an indoor-outdoor temperature difference on transient cross-ventilation. Build. Environ. 168, 106447 https://doi.org/10.1016/j.buildenv.2019.106447.

De Dear, R.J., Arens, E., Hui, Z., Oguro, M., 1997. Convective and radiative heat transfer coefficients for individual human body segments. Int. J. Biometeorol. 40 (3), 141–156.

Eliasson, I., Offerle, B., Grimmond, C., Lindqvist, S., 2006. Wind fields and turbulence statistics in an urban street canyon. Atmos. Environ. 40 (1), 1–16.

Embid, P.F., Majda, A.J., 2006. Low Froude number limiting dynamics for stably stratified flow with small or finite Rossby numbers. Geophys. Astrophys. Fluid Dynam. 87 (1–2), 1–50. https://doi.org/10.1080/03091929808208993.

Esfeh, M.K., Sohankar, A., Shahsavari, A.R., Rastan, M.R., Ghodrat, M., Nili, M., 2021. Experimental and numerical evaluation of wind-driven natural ventilation of a curved roof for various wind angles. Build. Environ. 205, 108275 https://doi.org/10.1016/j.buildenv.2021.108275.

Etheridge, D., 2011. Natural Ventilation of Buildings: Theory, Measurement and Design. John Wiley & Sons.

Fan, Y., Li, Y., Bejan, A., Wang, Y., Yang, X., 2017. Horizontal extent of the urban heat dome flow. Sci. Rep. 7 (1), 11681. https://doi.org/10.1038/s41598-017-09917-4.

Fan, Y., Li, Y., Yin, S., 2018. Interaction of multiple urban heat island circulations under idealised settings. Build. Environ. 134, 10–20. https://doi.org/10.1016/j.buildenv.2018.02.028.

Fan, Y., Wang, Q., Yin, S., Li, Y., 2019. Effect of city shape on urban wind patterns and convective heat transfer in calm and stable background conditions. Build. Environ. 162, 106288.

Fan, Y., Wang, Q., Ge, J., Li, Y., 2020. Conditions for transition from a plume to a dome above a heated horizontal area. Int. J. Heat Mass Transf. 156, 119868 https://doi.org/10.1016/j.ijheatmasstransfer.2020.119868.

Fan, Y., Hunt, J., Wang, Q., Li, Y., 2021a. Inversion breakup over different shapes of urban areas. Build. Environ. 190, 107548 https://doi.org/10.1016/j.buildenv.2020.107548.

Fan, Y., Zhao, Y., Torres, J.F., Xu, F., Lei, C., Li, Y., Carmeliet, J., 2021b. Natural convection over vertical and horizontal heated flat surfaces: a review of recent progress focusing on underpinnings and implications for heat transfer and environmental applications. Phys. Fluids 33 (10), 101301.

Fellini, S., Ridolfi, L., Salizzoni, P., 2020. Street canyon ventilation: combined effect of cross-section geometry and wall heating. Q. J. R. Meteorol. Soc. 146 (730), 2347–2367.

Fellini, S., Marro, M., Del Ponte, A.V., Barulli, M., Soulhac, L., Ridolfi, L., Salizzoni, P., 2022. High resolution wind-tunnel investigation about the effect of street trees on pollutant concentration and street canyon ventilation. Build. Environ. 109763.

Fiala, D., Havenith, G., Bröde, P., Kampmann, B., Jendritzky, G., 2012. UTCI-Fiala multi-node model of human heat transfer and temperature regulation. Int. J. Biometeorol. 56 (3), 429–441.
Franke, J., Hellsten, A., Schlünzen, K.H., Carissimo, B., 2007. Best practice guideline for the CFD simulation of flows in the urban environment - a summary. In: 11th Conference on Harmonisation within Atmospheric Dispersion Modelling for Regulatory Purposes, Cambridge, UK, July 2007 Cambridge Environmental Research Consultants.
Gaber, N., Ibrahim, A., Rashad, A.B., Wahba, E., El-Sayad, Z., Bakr, A.F., 2020. Improving pedestrian micro-climate in urban canyons: city Center of Alexandria, Egypt. Urban Clim. 34, 100670 https://doi.org/10.1016/j.uclim.2020.100670.
Gagge, A., Stolwijk, J., Nishi, Y., 1972. An effective temperature scale based on a simple model of human physiological regulatiry response. Mem. Fac. Eng. Hokkaido Univ. 13 (Suppl), 21–36.
Gaheen, O.A., Benini, E., Khalifa, M.A., El-Salamony, M.E., Aziz, M.A., 2021. Experimental investigation on the convection heat transfer enhancement for heated cylinder using pulsated flow. Therm. Sci. Eng. Progr. 26, 101055 https://doi.org/10.1016/j.tsep.2021.101055.
Gailis, R., Hill, A., 2006. A wind-tunnel simulation of plume dispersion within a large array of obstacles. Bound.-Layer Meteorol. 119 (2), 289–338.
Gallo, A., Marzo, A., Fuentealba, E., Alonso, E., 2017. High flux solar simulators for concentrated solar thermal research: a review. Renew. Sust. Energ. Rev. 77, 1385–1402. https://doi.org/10.1016/j.rser.2017.01.056.
Gao, H., Liu, J., Lin, P., Li, C., Xiao, Y., Hu, G., 2022. Pedestrian level wind flow field of elevated tall buildings with dense tandem arrangement. Build. Environ. 226, 109745 https://doi.org/10.1016/j.buildenv.2022.109745.
Garbero, V., Salizzoni, P., Soulhac, L., 2010. Experimental study of pollutant dispersion within a network of streets. Bound.-Layer Meteorol. 136 (3), 457–487.
García-Sánchez, C., van Beeck, J., Gorlé, C., 2018. Predictive large eddy simulations for urban flows: challenges and opportunities. Build. Environ. 139, 146–156. https://doi.org/10.1016/j.buildenv.2018.05.007.
Golubić, D., Meile, W., Brenn, G., Kozmar, H., 2020. Wind-tunnel analysis of natural ventilation in a generic building in sheltered and unsheltered conditions: impact of Reynolds number and wind direction. J. Wind Eng. Ind. Aerodyn. 207, 104388 https://doi.org/10.1016/j.jweia.2020.104388.
Gong, J., Cheng, K.X., Liu, H., Chew, L.W., Lee, P.S., 2022. A novel staggered split absorber design for enhanced solar chimney performance. Build. Environ. 224, 109569 https://doi.org/10.1016/j.buildenv.2022.109569.
Gromke, C., 2011. A vegetation modeling concept for building and environmental aerodynamics wind tunnel tests and its application in pollutant dispersion studies. Environ. Pollut. 159 (8-9), 2094–2099. https://doi.org/10.1016/j.envpol.2010.11.012.
Gromke, C., 2018. Wind tunnel model of the forest and its Reynolds number sensitivity. J. Wind Eng. Ind. Aerodyn. 175, 53–64. https://doi.org/10.1016/j.jweia.2018.01.036.
Gromke, C., Blocken, B., 2015. Influence of avenue-trees on air quality at the urban neighborhood scale. Part II: traffic pollutant concentrations at pedestrian level. Environ. Pollut. 196, 176–184. https://doi.org/10.1016/j.envpol.2014.10.015.
Gromke, C., Ruck, B., 2007. Influence of trees on the dispersion of pollutants in an urban street canyon—experimental investigation of the flow and concentration field. Atmos. Environ. 41 (16), 3287–3302.
Gromke, C., Ruck, B., 2008. Aerodynamic modelling of trees for small-scale wind tunnel studies. Forestry 81 (3), 243–258. https://doi.org/10.1093/forestry/cpn027.
Gromke, C., Ruck, B., 2009. On the impact of trees on dispersion processes of traffic emissions in street canyons. Bound.-Layer Meteorol. 131 (1), 19–34.
Gromke, C., Ruck, B., 2012. Pollutant concentrations in street canyons of different aspect ratio with avenues of trees for various wind directions. Bound.-Layer Meteorol. 144 (1), 41–64.
Gromke, C., Ruck, B., 2018. On wind forces in the forest-edge region during extreme-gust passages and their implications for damage patterns. Bound.-Layer Meteorol. 168 (2), 269–288. https://doi.org/10.1007/s10546-018-0348-4.
Gromke, C., Jamarkattel, N., Ruck, B., 2016. Influence of roadside hedgerows on air quality in urban street canyons. Atmos. Environ. 139, 75–86. https://doi.org/10.1016/j.atmosenv.2016.05.014.
Groth, J., Johansson, A.V., 1988. Turbulence reduction by screens. J. Fluid Mech. 197, 139–155. https://doi.org/10.1017/S0022112088003209.
Grunert, F., Benndorf, D., Klingbeil, K., 1984. Neure Ergebnisse zum Aufbau von Schutzpflanzungen.
Guo, D., Yang, F., Shi, X., Li, Y., Yao, R., 2021. Numerical simulation and wind tunnel experiments on the effect of a cubic building on the flow and pollutant diffusion under stable stratification. Build. Environ. 205, 108222 https://doi.org/10.1016/j.buildenv.2021.108222.
Hajra, B., Stathopoulos, T., 2012. A wind tunnel study of the effect of downstream buildings on near-field pollutant dispersion. Build. Environ. 52, 19–31.
Hangan, H., Refan, M., Jubayer, C., Romanic, D., Parvu, D., LoTufo, J., Costache, A., 2017. Novel techniques in wind engineering. J. Wind Eng. Ind. Aerodyn. 171, 12–33.
Hao, Y., Kopp, G.A., Wu, C.-H., Gillmeier, S., 2020. A wind tunnel study of the aerodynamic characteristics of a scaled, aeroelastic, model tree. J. Wind Eng. Ind. Aerodyn. 197, 104088 https://doi.org/10.1016/j.jweia.2019.104088.
Harris, C.L., 1934. Influence of neighboring structures on the wind pressure on tall buildings. Bur. Stand. J. Res. 12, 103–117.
H'ng, Y.M., Ikegaya, N., Zaki, S.A., Hagishima, A., Mohammad, A.F., 2022. Wind-tunnel estimation of mean and turbulent wind speeds within canopy layer for urban campus. Urban Clim. 41, 101064 https://doi.org/10.1016/j.uclim.2021.101064.
Holmes, J.D., Carpenter, P., 1990. The effect of Jensen Number variations on the wind loads on a low-rise building. J. Wind Eng. Ind. Aerodyn. 36, 1279–1288. https://doi.org/10.1016/0167-6105(90)90124-U.
Huang, B., Li, Z., Gong, B., Zhang, Z., Shan, B., Pu, O., 2023. Study on the sandstorm load of low-rise buildings via wind tunnel testing. J. Build. Eng. 65, 105821 https://doi.org/10.1016/j.jobe.2022.105821.
Hunt, J., Poulton, E., Mumford, J., 1976. The effects of wind on people; new criteria based on wind tunnel experiments. Build. Environ. 11 (1), 15–28.
Hunt, J., Richards, K., Brighton, P., 1988. Stably stratified shear flow over low hills. Q. J. R. Meteorol. Soc. 114 (482), 859–886.
James Lo, L., Banks, D., Novoselac, A., 2013. Combined wind tunnel and CFD analysis for indoor airflow prediction of wind-driven cross ventilation. Build. Environ. 60, 12–23. https://doi.org/10.1016/j.buildenv.2012.10.022.
Jeanjean, A.P.R., Hinchliffe, G., McMullan, W.A., Monks, P.S., Leigh, R.J., 2015. A CFD study on the effectiveness of trees to disperse road traffic emissions at a city scale. Atmos. Environ. 120, 1–14. https://doi.org/10.1016/j.atmosenv.2015.08.003.
Ji, L., Tan, H., Kato, S., Bu, Z., Takahashi, T., 2011. Wind tunnel investigation on influence of fluctuating wind direction on cross natural ventilation. Build. Environ. 46 (12), 2490–2499. https://doi.org/10.1016/j.buildenv.2011.06.006.
Joselin Herbert, G.M., Iniyan, S., Sreevalsan, E., Rajapandian, S., 2007. A review of wind energy technologies. Renew. Sust. Energ. Rev. 11 (6), 1117–1145. https://doi.org/10.1016/j.rser.2005.08.004.
Kanda, I., Uehara, K., Yamao, Y., Yoshikawa, Y., Morikawa, T., 2006. A wind-tunnel study on exhaust gas dispersion from road vehicles—Part I: velocity and concentration fields behind single vehicles. J. Wind Eng. Ind. Aerodyn. 94 (9), 639–658. https://doi.org/10.1016/j.jweia.2005.12.003.
Kareem, A., 2020. Emerging frontiers in wind engineering: computing, stochastics, machine learning and beyond. J. Wind Eng. Ind. Aerodyn. 206, 104320.
Kastner-Klein, P., Fedorovich, E., Rotach, M., 2001. A wind tunnel study of organised and turbulent air motions in urban street canyons. J. Wind Eng. Ind. Aerodyn. 89 (9), 849–861.
Kawai, T., Kanda, M., 2010. Urban energy balance obtained from the comprehensive outdoor scale model experiment. Part I: basic features of the surface energy balance. J. Appl. Meteorol. Climatol. 49 (7), 1341–1359.
Khaled, M.F., Aly, A.M., 2022. Assessing aerodynamic loads on low-rise buildings considering Reynolds number and turbulence effects: a review. Adv. Aerodyn. 4 (1), 24. https://doi.org/10.1186/s42774-022-00114-0.
Klausmann, K., Ruck, B., 2017. Drag reduction of circular cylinders by porous coating on the leeward side. J. Fluid Mech. 813, 382–411. https://doi.org/10.1017/jfm.2016.757.
Klein, P., Leitl, B., Schatzmann, M., 2011. Concentration fluctuations in a downtown urban area. Part II: analysis of Joint Urban 2003 wind-tunnel measurements. Environ. Fluid Mech. 11 (1), 43–60.

Kubilay, A., Allegrini, J., Strebel, D., Zhao, Y., Derome, D., Carmeliet, J., 2020. Advancement in urban climate modelling at local scale: urban heat island mitigation and building cooling demand. Atmosphere 11 (12), 1313.
Kulkarni, V., Sahoo, N., Chavan, S.D., 2011. Simulation of honeycomb–screen combinations for turbulence management in a subsonic wind tunnel. J. Wind Eng. Ind. Aerodyn. 99 (1), 37–45. https://doi.org/10.1016/j.jweia.2010.10.006.
Lareau, N.P., Crosman, E., Whiteman, C.D., Horel, J.D., Hoch, S.W., Brown, W.O., Horst, T.W., 2013. The persistent cold-air pool study. Bull. Am. Meteorol. Soc. 94 (1), 51–63.
Largeron, Y., Staquet, C., 2016. Persistent inversion dynamics and wintertime PM10 air pollution in Alpine valleys. Atmos. Environ. 135, 92–108. https://doi.org/10.1016/j.atmosenv.2016.03.045.
Le Sant, Y., Marchand, M., Millan, P., Fontaine, J., 2002. An overview of infrared thermography techniques used in large wind tunnels. Aerosp. Sci. Technol. 6 (5), 355–366.
Li, C., Ito, K., 2014. Numerical and experimental estimation of convective heat transfer coefficient of human body under strong forced convective flow. J. Wind Eng. Ind. Aerodyn. 126, 107–117.
Li, X.-X., Liu, C.-H., Leung, D.Y.C., Lam, K.M., 2006. Recent progress in CFD modelling of wind field and pollutant transport in street canyons. Atmos. Environ. 40 (29), 5640–5658. https://doi.org/10.1016/j.atmosenv.2006.04.055.
Li, H., Zhao, Y., Liu, J., Carmeliet, J., 2021a. Physics-based stitching of multi-FOV PIV measurements for urban wind fields. Build. Environ. 205, 108306 https://doi.org/10.1016/j.buildenv.2021.108306.
Li, Z., Ming, T., Liu, S., Peng, C., de Richter, R., Li, W., Zhang, H., Wen, C.-Y., 2021b. Review on pollutant dispersion in urban areas-Part A: effects of mechanical factors and urban morphology. Build. Environ. 190, 107534 https://doi.org/10.1016/j.buildenv.2020.107534.
Li, H., Zhao, Y., Sützl, B., Kubilay, A., Carmeliet, J., 2022a. Impact of green walls on ventilation and heat removal from street canyons: coupling of thermal and aerodynamic resistance. Build. Environ. 214, 108945 https://doi.org/10.1016/j.buildenv.2022.108945.
Li, J., Hu, J., Lin, M., 2022b. A flexibly controllable high-flux solar simulator for concentrated solar energy research from extreme magnitudes to uniform distributions. Renew. Sust. Energ. Rev. 157, 112084 https://doi.org/10.1016/j.rser.2022.112084.
Lim, H., Hertwig, D., Grylls, T., Gough, H., Reeuwijk, M.V., Grimmond, S., Vanderwel, C., 2022. Pollutant dispersion by tall buildings: laboratory experiments and Large-Eddy Simulation. Exp. Fluids 63 (6), 1–20.
Lin, Y., Hang, J., Yang, H., Chen, L., Chen, G., Ling, H., Sandberg, M., Claesson, L., Lam, C.K.C., 2021. Investigation of the Reynolds number independence of cavity flow in 2D street canyons by wind tunnel experiments and numerical simulations. Build. Environ. 201, 107965 https://doi.org/10.1016/j.buildenv.2021.107965.
Linden, P.F., 1999. The fluid mechanics of natural ventilation. Annu. Rev. Fluid Mech. 31 (1), 201–238.
Linden, P.F., Lane-Serff, G.F., Smeed, D.A., 1990. Emptying filling boxes: the fluid mechanics of natural ventilation. J. Fluid Mech. 212, 309–335. https://doi.org/10.1017/S0022112090001987.
Liu, X.P., Niu, J.L., Kwok, K.C.S., Wang, J.H., Li, B.Z., 2010. Investigation of indoor air pollutant dispersion and cross-contamination around a typical high-rise residential building: wind tunnel tests. Build. Environ. 45 (8), 1769–1778. https://doi.org/10.1016/j.buildenv.2010.02.003.
Llaguno-Munitxa, M., Bou-Zeid, E., Hultmark, M., 2017. The influence of building geometry on street canyon air flow: validation of large eddy simulations against wind tunnel experiments. J. Wind Eng. Ind. Aerodyn. 165, 115–130.
Lu, J., Arya, S.P., Snyder, W.H., Lawson, R.E., 1997a. A laboratory study of the urban heat island in a calm and stably stratified environment. Part I: temperature field. J. Appl. Meteorol. Climatol. 36 (10), 1377–1391.
Lu, J., Arya, S.P., Snyder, W.H., Lawson, R.E., 1997b. A laboratory study of the urban heat island in a calm and stably stratified environment. Part II: velocity field. J. Appl. Meteorol. Climatol. 36 (10), 1392–1402.
Luo, N., Weng, W., Fu, M., Yang, J., Han, Z., 2014. Experimental study of the effects of human movement on the convective heat transfer coefficient. Exp. Thermal Fluid Sci. 57, 40–56.
Macdonald, R., Griffiths, R., Hall, D., 1998. A comparison of results from scaled field and wind tunnel modelling of dispersion in arrays of obstacles. Atmos. Environ. 32 (22), 3845–3862.
Manickathan, L., Defraeye, T., Allegrini, J., Derome, D., Carmeliet, J., 2018. Comparative study of flow field and drag coefficient of model and small natural trees in a wind tunnel. Urban For. Urban Green. 35, 230–239. https://doi.org/10.1016/j.ufug.2018.09.011.
Manickathan, L., Defraeye, T., Carl, S., Richter, H., Allegrini, J., Derome, D., Carmeliet, J., 2022. A study on diurnal microclimate hysteresis and plant morphology of a Buxus sempervirens using PIV, infrared thermography, and X-ray imaging. Agric. For. Meteorol. 313, 108722 https://doi.org/10.1016/j.agrformet.2021.108722.
Marro, M., Salizzoni, P., Cierco, F.-X., Korsakissok, I., Danzi, E., Soulhac, L., 2014. Plume rise and spread in buoyant releases from elevated sources in the lower atmosphere. Environ. Fluid Mech. 14 (1), 201–219.
Marro, M., Gamel, H., Méjean, P., Correia, H., Soulhac, L., Salizzoni, P., 2020. High-frequency simultaneous measurements of velocity and concentration within turbulent flows in wind-tunnel experiments. Exp. Fluids 61 (12), 1–13.
Marucci, D., Carpentieri, M., 2019. Effect of local and upwind stratification on flow and dispersion inside and above a bi-dimensional street canyon. Build. Environ. 156, 74–88.
Marucci, D., Carpentieri, M., 2020a. Dispersion in an array of buildings in stable and convective atmospheric conditions. Atmos. Environ. 222, 117100.
Marucci, D., Carpentieri, M., 2020b. Stable and convective boundary-layer flows in an urban array. J. Wind Eng. Ind. Aerodyn. 200, 104140.
Masson, V., 2006. Urban surface modeling and the meso-scale impact of cities. Theor. Appl. Climatol. 84 (1), 35–45.
Masson, V., Lemonsu, A., Hidalgo, J., Voogt, J., 2020. Urban climates and climate change. Annu. Rev. Environ. Resour. 45 (1), 411–444. https://doi.org/10.1146/annurev-environ-012320-083623.
McPhail, M.J., Fontaine, A.A., Krane, M.H., Goss, L., Crafton, J., 2015. Correcting for color crosstalk and chromatic aberration in multicolor particle shadow velocimetry. Meas. Sci. Technol. 26 (2), 025302 https://doi.org/10.1088/0957-0233/26/2/025302.
Mei, S.-J., Yuan, C., 2021. Analytical and numerical study on transient urban street air warming induced by anthropogenic heat emission. Energy Build. 231, 110613 https://doi.org/10.1016/j.enbuild.2020.110613.
Mei, S.-J., Yuan, C., 2022. Urban buoyancy-driven air flow and modelling method: a critical review. Build. Environ. 210, 108708 https://doi.org/10.1016/j.buildenv.2021.108708.
Mei, S.-J., Zhao, Y., Talwar, T., Carmeliet, J., Yuan, C., 2023. Neighborhood scale traffic pollutant dispersion subject to different wind-buoyancy ratios: a LES case study in Singapore. Build. Environ. 228, 109831 https://doi.org/10.1016/j.buildenv.2022.109831.
Merlier, L., Jacob, J., Sagaut, P., 2018. Lattice-Boltzmann large-eddy simulation of pollutant dispersion in street canyons including tree planting effects. Atmos. Environ. 195, 89–103. https://doi.org/10.1016/j.atmosenv.2018.09.040.
Meroney, R., 2004. Wind tunnel and numerical simulation of pollution dispersion: a hybrid approach. In: Paper for Invited Lecture at the Croucher Advanced Study Institute. Hong Kong University of Science and Technology, pp. 6–10.
Meroney, R.N., 2016. Ten questions concerning hybrid computational/physical model simulation of wind flow in the built environment. Build. Environ. 96, 12–21. https://doi.org/10.1016/j.buildenv.2015.11.005.
Meroney, R.N., Pavageau, M., Rafailidis, S., Schatzmann, M., 1996. Study of line source characteristics for 2-D physical modelling of pollutant dispersion in street canyons. J. Wind Eng. Ind. Aerodyn. 62 (1), 37–56.
Mirzaei, P.A., Carmeliet, J., 2015. Influence of the underneath cavity on buoyant-forced cooling of the integrated photovoltaic panels in building roof: a thermography study. Prog. Photovolt. Res. Appl. 23 (1), 19–29. https://doi.org/10.1002/pip.2390.
Mirzaei, P.A., Paterna, E., Carmeliet, J., 2014. Investigation of the role of cavity airflow on the performance of building-integrated photovoltaic panels. Sol. Energy 107, 510–522. https://doi.org/10.1016/j.solener.2014.05.003.
Mo, Z., Liu, C.-H., 2018. Wind tunnel measurements of pollutant plume dispersion over hypothetical urban areas. Build. Environ. 132, 357–366.
Mo, Z., Liu, C.-H., 2023. Inertial and roughness sublayer flows over real urban morphology: a comparison of wind tunnel experiment and large-eddy simulation. Urban Clim. 49, 101530 https://doi.org/10.1016/j.uclim.2023.101530.

Moayedi, S.H., Hassanzadeh, S., 2022. An LES study of aerodynamic effect of trees on traffic pollutant dispersion in an ideal street canyon. Europ. Phys. J. Plus 137 (7). https://doi.org/10.1140/epjp/s13360-022-03004-y.
Moonen, P., Defraeye, T., Dorer, V., Blocken, B., Carmeliet, J., 2012. Urban physics: effect of the micro-climate on comfort, health and energy demand. Front. Architect. Res. 1 (3), 197–228.
Moonen, P., Gromke, C., Dorer, V., 2013. Performance assessment of Large Eddy Simulation (LES) for modeling dispersion in an urban street canyon with tree planting. Atmos. Environ. 75, 66–76. https://doi.org/10.1016/j.atmosenv.2013.04.016.
Morakinyo, T.E., Lam, Y.F., 2016. Study of traffic-related pollutant removal from street canyon with trees: dispersion and deposition perspective. Environ. Sci. Pollut. Res. Int. 23 (21), 21652–21668. https://doi.org/10.1007/s11356-016-7322-9.
Mouzourides, P., Marakkos, C., Neophytou, M.K.-A., 2022. Urban street canyon flows under combined wind forcing and thermal buoyancy. Phys. Fluids 34 (7), 076606. https://doi.org/10.1063/5.0090642.
Murakami, S., 1990. Computational wind engineering. J. Wind Eng. Ind. Aerodyn. 36, 517–538. https://doi.org/10.1016/0167-6105(90)90335-A.
Murakami, S., Deguchi, K., 1981. New criteria for wind effects on pedestrians. J. Wind Eng. Ind. Aerodyn. 7 (3), 289–309.
Nathan, P., Manning, R., Birch, D.M., 2021. Dynamic compensation of ultra-low-range pressure sensors. IEEE Sensors J. 21 (9), 11094–11100.
Nazarian, N., Martilli, A., Kleissl, J., 2018. Impacts of realistic urban heating, Part I: spatial variability of mean flow, turbulent exchange and pollutant dispersion. Bound.-Layer Meteorol. 166 (3), 367–393.
Niedźwiedź, T., Łupikasza, E.B., Małarzewski, Ł., Budzik, T., 2021. Surface-based nocturnal air temperature inversions in southern Poland and their influence on PM10 and PM2.5 concentrations in Upper Silesia. Theor. Appl. Climatol. 146 (3–4), 897–919. https://doi.org/10.1007/s00704-021-03752-4.
Ning, G., Wang, S., Yim, S.H.L., Li, J., Hu, Y., Shang, Z., Wang, J., Wang, J., 2018. Impact of low-pressure systems on winter heavy air pollution in the northwest Sichuan Basin, China. Atmos. Chem. Phys. 18 (18), 13601–13615. https://doi.org/10.5194/acp-18-13601-2018.
Nosek, Š., Kukačka, L., Kellnerová, R., Jurčáková, K., Jaňour, Z., 2016. Ventilation processes in a three-dimensional street canyon. Bound.-Layer Meteorol. 159 (2), 259–284.
Nosek, Š., Jaňour, Z., Janke, D., Yi, Q., Aarnink, A., Calvet, S., Hassouna, M., Jakubcová, M., Demeyer, P., Zhang, G., 2021. Review of wind tunnel modelling of flow and pollutant dispersion within and from naturally ventilated livestock buildings. Appl. Sci. 11 (9), 3783.
Offerle, B., Eliasson, I., Grimmond, C., Holmer, B., 2007. Surface heating in relation to air temperature, wind and turbulence in an urban street canyon. Bound.-Layer Meteorol. 122 (2), 273–292.
Ogawa, Y., Diosey, P., Uehara, K., Ueda, H., 1981. A wind tunnel for studying the effects of thermal stratification in the atmosphere. Atmosph. Environ. (1967) 15 (5), 807–821.
Ogawa, Y., Diosey, P., Uehara, K., Ueda, H., 1985. Wind tunnel observation of flow and diffusion under stable stratification. Atmosph. Environ. (1967) 19 (1), 65–74.
Oliveira, A.V.M., Gaspar, A.R., Francisco, S.C., Quintela, D.A., 2014. Analysis of natural and forced convection heat losses from a thermal manikin: comparative assessment of the static and dynamic postures. J. Wind Eng. Ind. Aerodyn. 132, 66–76.
Pađen, I., García-Sánchez, C., Ledoux, H., 2022. Towards automatic reconstruction of 3D city models tailored for urban flow simulations. Front. Built Environ. 8 https://doi.org/10.3389/fbuil.2022.899332.
Pappa, V., Bouris, D., Theurer, W., Gromke, C., 2023. A wind tunnel study of aerodynamic effects of façade and roof greening on air exchange from a cubic building. Build. Environ. 231, 110023 https://doi.org/10.1016/j.buildenv.2023.110023.
Pavageau, M., Schatzmann, M., 1999. Wind tunnel measurements of concentration fluctuations in an urban street canyon. Atmos. Environ. 33 (24-25), 3961–3971.
Perry, S., Heist, D., Brouwer, L., Monbureau, E., Brixey, L., 2016. Characterization of pollutant dispersion near elongated buildings based on wind tunnel simulations. Atmos. Environ. 142, 286–295.
Plate, E., 1982. Windkanalmodellierung von ausbreitungsvorgangen in stadtgebieten, kolloq-uiumsbericht abgasbelastungen durch den strabenverkehr. Verlag TUV Rheiland.
Plate, E.J., 1999. Methods of investigating urban wind fields—physical models. Atmos. Environ. 33 (24–25), 3981–3989.
Pournazeri, S., Princevac, M., Venkatram, A., 2012. Scaling of building affected plume rise and dispersion in water channels and wind tunnels—Revisit of an old problem. J. Wind Eng. Ind. Aerodyn. 103, 16–30.
Princevac, M., Fernando, H., 2008. Morning breakup of cold pools in complex terrain. J. Fluid Mech. 616, 99–109.
Raffaele, L., van Beeck, J., Bruno, L., 2021. Wind-sand tunnel testing of surface-mounted obstacles: similarity requirements and a case study on a Sand Mitigation Measure. J. Wind Eng. Ind. Aerodyn. 214, 104653 https://doi.org/10.1016/j.jweia.2021.104653.
Renné, D.S., 2016. Resource Assessment and Site Selection for Solar Heating and Cooling Systems, pp. 13–41. https://doi.org/10.1016/b978-0-08-100301-5.00002-3.
Reuten, C., 2006. Scaling and Kinematics of Daytime Slope Flow Systems.
Ricci, A., Burlando, M., Freda, A., Repetto, M.P., 2017a. Wind tunnel measurements of the urban boundary layer development over a historical district in Italy. Build. Environ. 111, 192–206.
Ricci, A., Kalkman, I., Blocken, B., Burlando, M., Freda, A., Repetto, M., 2017b. Local-scale forcing effects on wind flows in an urban environment: Impact of geometrical simplifications. J. Wind Eng. Ind. Aerodyn. 170, 238–255.
Ricci, A., Guasco, M., Caboni, F., Orlanno, M., Giachetta, A., Repetto, M., 2022. Impact of surrounding environments and vegetation on wind comfort assessment of a new tower with vertical green park. Build. Environ. 207, 108409.
Richter, A., Ruck, B., Mohr, S., Kunz, M., 2018. Interaction of severe convective gusts with a street canyon. Urban Clim. 23, 71–90. https://doi.org/10.1016/j.uclim.2016.11.003.
Robins, A., Castro, I., Hayden, P., Steggel, N., Contini, D., Heist, D., John Taylor, T., 2001. A wind tunnel study of dense gas dispersion in a stable boundary layer over a rough surface. Atmos. Environ. 35 (13), 2253–2263. https://doi.org/10.1016/S1352-2310(01)00073-5.
Salim, S.M., Cheah, S.C., Chan, A., 2011. Numerical simulation of dispersion in urban street canyons with avenue-like tree plantings: comparison between RANS and LES. Build. Environ. 46 (9), 1735–1746. https://doi.org/10.1016/j.buildenv.2011.01.032.
Salizzoni, P., Soulhac, L., Mejean, P., 2009. Street canyon ventilation and atmospheric turbulence. Atmos. Environ. 43 (32), 5056–5067.
Sellers, P.J., Dickinson, R.E., Randall, D.A., Betts, A.K., Hall, F.G., Berry, J.A., Collatz, G.J., Denning, A.S., Mooney, H.A., Nobre, C.A., Sato, N., Field, C.B., Henderson-Sellers, A., 1997. Modeling the exchanges of energy, water, and carbon between continents and the atmosphere. Science 275 (5299), 502–509. https://doi.org/10.1126/science.275.5299.502.
Shaw, R., 1985. The dissipation of turbulence in plant canopies. In: 7th Symp. American Meteorol. Society on Turbulence and Diffusion, 1985, p. 11.
Shirzadi, M., Tominaga, Y., Mirzaei, P.A., 2019. Wind tunnel experiments on cross-ventilation flow of a generic sheltered building in urban areas. Build. Environ. 158, 60–72. https://doi.org/10.1016/j.buildenv.2019.04.057.
Shu, C., Wang, L., Mortezazadeh, M., 2020. Dimensional analysis of Reynolds independence and regional critical Reynolds numbers for urban aerodynamics. J. Wind Eng. Ind. Aerodyn. 203, 104232 https://doi.org/10.1016/j.jweia.2020.104232.
Simiu, E., Yeo, D., 2019. Wind Effects on Structures: Modern Structural Design for Wind. John Wiley & Sons.
Snyder, W.H., 1981. Guideline for Fluid Modeling of Atmospheric Diffusion. Environmental Sciences Research Laboratory, Office of Research and ….
Snyder, W.H., 2001. Wind-tunnel study of entrainment in two-dimensional dense-gas plumes at the EPA's fluid modeling facility. Atmos. Environ. 35 (13), 2285–2304. https://doi.org/10.1016/S1352-2310(00)00214-4.
Solari, G., 2019. Wind Science and Engineering: Origins, Developments, Fundamentals and Advancements. Springer.
Solari, G., Burlando, M., Repetto, M.P., 2020. Detection, simulation, modelling and loading of thunderstorm outflows to design wind-safer and cost-efficient structures. J. Wind Eng. Ind. Aerodyn. 200, 104142.
Song, J., Fan, S., Lin, W., Mottet, L., Woodward, H., Davies Wykes, M., Arcucci, R., Xiao, D., Debay, J.-E., ApSimon, H., 2018. Natural ventilation in cities: the implications of fluid mechanics. Build. Res. Inf. 46 (8), 809–828.
Stacey, G., Belcher, R., Wood, C., Gardiner, B., 1994. Wind flows and forces in a model spruce forest. Bound.-Layer Meteorol. 69 (3), 311–334.

Stathopoulos, T., 1997. Computational wind engineering: Past achievements and future challenges. J. Wind Eng. Ind. Aerodyn. 67-68, 509–532. https://doi.org/10.1016/S0167-6105(97)00097-4.
Stathopoulos, T., Surry, D., 1983. Scale effects in wind tunnel testing of low buildings. J. Wind Eng. Ind. Aerodyn. 13 (1-3), 313–326.
Stathopoulos, T., Wu, H., Zacharias, J., 2004. Outdoor human comfort in an urban climate. Build. Environ. 39 (3), 297–305. https://doi.org/10.1016/j.buildenv.2003.09.001.
Stathopoulos, T., Alrawashdeh, H., Al-Quraan, A., Blocken, B., Dilimulati, A., Paraschivoiu, M., Pilay, P., 2018. Urban wind energy: some views on potential and challenges. J. Wind Eng. Ind. Aerodyn. 179, 146–157.
Stull, R.B., 1988. An Introduction to Boundary Layer Meteorology. Springer Science & Business Media.
Tanabe, S.-I., Arens, E.A., Bauman, F., Zhang, H., Madsen, T., 1994. Evaluating Thermal Environments by Using a Thermal Manikin with Controlled Skin Surface Temperature.
Tawfik, M., Tonnellier, X., Sansom, C., 2018. Light source selection for a solar simulator for thermal applications: a review. Renew. Sust. Energ. Rev. 90, 802–813. https://doi.org/10.1016/j.rser.2018.03.059.
Tecle, A., Bitsuamlak, G.T., Jiru, T.E., 2013. Wind-driven natural ventilation in a low-rise building: a Boundary Layer Wind Tunnel study. Build. Environ. 59, 275–289. https://doi.org/10.1016/j.buildenv.2012.08.026.
Tominaga, Y., Stathopoulos, T., 2016. Ten questions concerning modeling of near-field pollutant dispersion in the built environment. Build. Environ. 105, 390–402.
Tominaga, Y., Mochida, A., Yoshie, R., Kataoka, H., Nozu, T., Yoshikawa, M., Shirasawa, T., 2008. AIJ guidelines for practical applications of CFD to pedestrian wind environment around buildings. J. Wind Eng. Ind. Aerodyn. 96 (10), 1749–1761. https://doi.org/10.1016/j.jweia.2008.02.058.
Tsalicoglou, C., Allegrini, J., Carmeliet, J., 2020. Non-isothermal flow between heated building models. J. Wind Eng. Ind. Aerodyn. 204, 104248.
Tse, K.T., Zhang, X., Weerasuriya, A.U., Li, S.W., Kwok, K.C.S., Mak, C.M., Niu, J., 2017. Adopting 'lift-up' building design to improve the surrounding pedestrian-level wind environment. Build. Environ. 117, 154–165. https://doi.org/10.1016/j.buildenv.2017.03.011.
Uehara, K., Murakami, S., Oikawa, S., Wakamatsu, S., 2000. Wind tunnel experiments on how thermal stratification affects flow in and above urban street canyons. Atmos. Environ. 34 (10), 1553–1562. https://doi.org/10.1016/S1352-2310(99)00410-0.
van der Laan, M.P., Kelly, M., Floors, R., Peña, A., 2020. Rossby number similarity of an atmospheric RANS model using limited-length-scale turbulence closures extended to unstable stratification. Wind Energy Sci. 5 (1), 355–374. https://doi.org/10.5194/wes-5-355-2020.
Vanderwel, C., Tavoularis, S., 2014. On the accuracy of PLIF measurements in slender plumes. Exp. Fluids 55 (8), 1801. https://doi.org/10.1007/s00348-014-1801-x.
Vidali, C., 2021. Atmospheric Dispersion of a Heavy Gas Release from an Elevated Source. Lyon.
Vidali, C., Marro, M., Correia, H., Gostiaux, L., Jallais, S., Houssin, D., Vyazmina, E., Salizzoni, P., 2022. Wind-tunnel experiments on atmospheric heavy gas dispersion: metrological aspects. Exp. Thermal Fluid Sci. 130, 110495.
Vosper, S.B., Brown, A.R., 2008. Numerical simulations of sheltering in valleys: the formation of nighttime cold-air pools. Bound.-Layer Meteorol. 127 (3), 429–448. https://doi.org/10.1007/s10546-008-9272-3.
Vranckx, S., Vos, P., Maiheu, B., Janssen, S., 2015. Impact of trees on pollutant dispersion in street canyons: a numerical study of the annual average effects in Antwerp, Belgium. Sci. Total Environ. 532, 474–483. https://doi.org/10.1016/j.scitotenv.2015.06.032.
Wang, H., Wang, Q., Yang, X., Chen, T., Lam, C.K.C., Zhang, M., Hang, J., 2021. Steady and unsteady turbulent flows and pollutant dispersion in 2D street canyons with novel boundary conditions and various Re numbers. Urban Clim. 39, 100973 https://doi.org/10.1016/j.uclim.2021.100973.
Wangsawijaya, D.D., Nicolai, C., Ganapathisubramani, B., 2022. Time-averaged velocity and scalar fields of the flow over and around a group of cylinders: a model experiment for canopy flows. Flow 2.
Warn, T., Bokhove, O., Shepherd, T.G., Vallis, G.K., 1995. Rossby number expansions, slaving principles, and balance dynamics. Q. J. R. Meteorol. Soc. 121 (523), 723–739. https://doi.org/10.1002/qj.49712152313.
Xia, Q., Niu, J., Liu, X., 2014. Dispersion of air pollutants around buildings: a review of past studies and their methodologies. Indoor Built Environ. 23 (2), 201–224.
Yassin, M., Kato, S., Ooka, R., Takahashi, T., Kouno, R., 2005. Field and wind-tunnel study of pollutant dispersion in a built-up area under various meteorological conditions. J. Wind Eng. Ind. Aerodyn. 93 (5), 361–382.
Yazid, A.W.M., Sidik, N.A.C., Salim, S.M., Saqr, K.M., 2014. A review on the flow structure and pollutant dispersion in urban street canyons for urban planning strategies. Simulation 90 (8), 892–916.
Yee, E., Biltoft, C.A., 2004. Concentration fluctuation measurements in a plume dispersing through a regular array of obstacles. Bound.-Layer Meteorol. 111 (3), 363–415.
Yee, E., Gailis, R.M., Hill, A., Hilderman, T., Kiel, D., 2006. Comparison of wind-tunnel and water-channel simulations of plume dispersion through a large array of obstacles with a scaled field experiment. Bound.-Layer Meteorol. 121 (3), 389–432.
Yen, J., Lei, C., Patterson, J.C., 2016. Simultaneous 2-colour LIF & PIV measurements of the boundary layer in a differentially heated cavity. In: 20th Australasian Fluid Mechanics Conference, Perth.
Yin, S., Fan, Y., Li, Y., Sandberg, M., Lam, K.-M., 2020. Experimental study of thermal plumes generated by a cluster of high-rise compact buildings under moderate background wind conditions. Build. Environ. 181, 107076 https://doi.org/10.1016/j.buildenv.2020.107076.
Ysebaert, T., Koch, K., Samson, R., Denys, S., 2021. Green walls for mitigating urban particulate matter pollution—a review. Urban For. Urban Green. 59, 127014 https://doi.org/10.1016/j.ufug.2021.127014.
Yu, L., Zhong, S., Bian, X., 2017. Multi-day valley cold-air pools in the western United States as derived from NARR. Int. J. Climatol. 37 (5), 2466–2476. https://doi.org/10.1002/joc.4858.
Yu, Y., Liu, J., Chauhan, K., de Dear, R., Niu, J., 2020. Experimental study on convective heat transfer coefficients for the human body exposed to turbulent wind conditions. Build. Environ. 169, 106533.
Yu, Y., de Dear, R., Chauhan, K., Niu, J., 2021. Impact of wind turbulence on thermal perception in the urban microclimate. J. Wind Eng. Ind. Aerodyn. 216, 104714.
Zhang, X., Tse, K.T., Weerasuriya, A.U., Li, S.W., Kwok, K.C.S., Mak, C.M., Niu, J., Lin, Z., 2017. Evaluation of pedestrian wind comfort near 'lift-up' buildings with different aspect ratios and central core modifications. Build. Environ. 124, 245–257. https://doi.org/10.1016/j.buildenv.2017.08.012.
Zhang, Y., Gu, Z., Yu, C.W., 2020. Impact factors on airflow and pollutant dispersion in urban street canyons and comprehensive simulations: a review. Curr. Poll. Rep. 6 (4), 425–439.
Zhao, Y., Chew, L.W., Kubilay, A., Carmeliet, J., 2020. Isothermal and non-isothermal flow in street canyons: a review from theoretical, experimental and numerical perspectives. Build. Environ. 184, 107163.
Zhao, Y., Li, H., Kubilay, A., Carmeliet, J., 2021. Buoyancy effects on the flows around flat and steep street canyons in simplified urban settings subject to a neutral approaching boundary layer: wind tunnel PIV measurements. Sci. Total Environ. 797, 149067.
Zhao, Y., Li, R., Feng, L., Wu, Y., Niu, J., Gao, N., 2022a. Boundary layer wind tunnel tests of outdoor airflow field around urban buildings: a review of methods and status. Renew. Sust. Energ. Rev. 167, 112717 https://doi.org/10.1016/j.rser.2022.112717.
Zhao, Y., Xue, Y., Mei, S., Chao, Y., Carmeliet, J., 2022b. Enhancement of heat removal from street canyons due to buoyant approaching flow: Water tunnel PIV-LIF measurements. Build. Environ. 226, 109757 https://doi.org/10.1016/j.buildenv.2022.109757.
Zhao, Y., Li, H., Bardhan, R., Kubilay, A., Li, Q., Carmeliet, J., 2023. The time-evolving impact of tree size on nighttime street canyon microclimate: wind tunnel modeling of aerodynamic effects and heat removal. Urban Clim. 49, 101528 https://doi.org/10.1016/j.uclim.2023.101528.
Zhou, X., Ouyang, Q., Lin, G., Zhu, Y., 2006. Impact of dynamic airflow on human thermal response. Indoor Air 16 (5), 348–355. https://doi.org/10.1111/j.1600-0668.2006.00430.x.
Zhu, X., Wang, X., Lei, L., Zhao, Y., 2022. The influence of roadside green belts and street canyon aspect ratios on air pollution dispersion and personal exposure. Urban Clim. 44, 101236 https://doi.org/10.1016/j.uclim.2022.101236.
Zou, J., Yu, Y., Liu, J., Niu, J., Chauhan, K., Lei, C., 2021. Field measurement of the urban pedestrian level wind turbulence. Build. Environ. 194, 107713.